Research

Check for updates

Author for correspondence:
Matjaž Perc
e-mail: matjaz.perc@gmail.com

Complex evolutionary dynamics due to punishment and free space in ecological multigames

Sayantan Nag Chowdhury[1], Srilena Kundu[1], Matjaž Perc[2,3,4,5] and Dibakar Ghosh[1]

[1]Physics and Applied Mathematics Unit, Indian Statistical Institute, 203 B. T. Road, Kolkata 700108, India
[2]Faculty of Natural Sciences and Mathematics, University of Maribor, Koroška cesta 160, 2000 Maribor, Slovenia
[3]Alma Mater Europaea, Slovenska ulica, 17, 2000 Maribor, Slovenia
[4]Department of Medical Research, China Medical University Hospital, China Medical University, Taichung, Taiwan
[5]Complexity Science Hub Vienna, Josefstädterstraße 39, 1080 Vienna, Austria

SNC, 0000-0002-0326-826X; MP, 0000-0002-3087-541X; DG, 0000-0003-4832-5210

The concurrence of ecological and evolutionary processes often arises as an integral part of various biological and social systems. We here study eco-evolutionary dynamics by adopting two paradigmatic metaphors of social dilemmas with contrasting outcomes. We use the Prisoner's Dilemma and Snowdrift games as the backbone of the proposed mathematical model. Since cooperation is a costly proposition in the face of the Darwinian theory of evolution, we go beyond the traditional framework by introducing punishment as an additional strategy. Punishers bare an additional cost from their own resources to try and discourage or prohibit free-riding from selfish defectors. Our model also incorporates the ecological signature of free space, which has an altruistic-like impact because it allows others to replicate and potentially thrive. We show that the consideration of these factors has broad implications for better understanding the emergent complex evolutionary dynamics. In particular, we report the simultaneous presence of different subpopulations through the spontaneous emergence of cyclic

dominance, and we determine various stationary points using traditional game-theoretic concepts and stability analysis.

1. Introduction

The dilemma of cooperation [1–4] under the Darwinian theory of evolution [5] has gained increasing attention among many interdisciplinary disciplines. Selfish individuals always look for higher personal benefits to maximize their welfare. This ubiquitous behaviour among those self-interested individuals leads to a scenario where it is risky to cooperate. Thus, the extinction of cooperation is perhaps the most unfortunate outcome that eventually leads to the tragedy of the commons [6]. However, in many real-world situations, including excessive usage of antibiotics [7], birds taking care of other's offspring [8], imperfect vaccination [9], grooming each other of vervet monkeys [10], acid rain [11], food sharing of the vampire bat [12] and many more, the emergence and persistence of cooperation is a widespread phenomenon in nature and social communities. Owing to the conflict of interests between the collective and selfish rationality, understanding the underlying mechanisms for the endurance of cooperation is a formidable challenge among different scientific communities [13,14]. The evolutionary game theory [15–17] is an insightful theoretical tool to resolve this long-standing pendulum of how cooperation evolves [18] contradictory to the much-celebrated Darwin's theory of evolution. Primarily game theory helps to recognize the consequences of strategic and economic decisions of humans [19]. Later, John Maynard Smith introduced evolutionary game theory, an application of the mathematical theory of games, to shed some light on the evolution of animal behaviour [16,20,21]. Nowadays, it has become an active interdisciplinary topic for understanding several social interactions in real-world systems [22], including the evolution of human language [23], host–parasite interactions [24], price decision [25], bacterial population dynamics [26] and strategy conflict in the form of dilemma [27], to name a few.

So under simplified assumptions, there are two types of individuals in society. One group continuously contributes to the common pool selflessly and helps to maintain the evolution of cooperation. On the other hand, another class of people always engages in some antisocial, selfish activities, posing threats to the collaborative efforts of cooperative behaviour. A few social games have been proposed based on these ideas. The paradigmatic examples are the Prisoner's Dilemma (PD) game [27] the Chicken or Snowdrift (SD) game [20,28] the Stag Hunt game [29] and so on. For the spreading of collective and cooperative habits, rewarding the cooperators [30–33] is an efficient approach for encouraging cooperative behaviour. However, rewarding cooperation may seem to be an expensive proposition in a large population of cooperators. Moreover, the positive incentives towards cooperators may fail to stabilize cooperation in a few cases [31]. Thus, punishing a population of cheaters may be a better proposal for promoting and maintaining cooperation instead of the tedious effort of taxing to reward cooperators who behaved properly. Punishing bad deeds ultimately helps to maintain the healthy functioning of societies and elevates the cooperative behaviour in populations. The effect of punishment on collective behaviours is immensely investigated in numerous empirical and theoretical studies among theorists and experimentalists [30–41]. Besides, other parameters exist in the social evolution, whose selfless act promotes the fitness of other individuals without expecting compensation for that action [42,43]. One of such altruistic variables is free space. Lots of earlier investigations deal with free space using the concept of mobility from different perspectives [44–54]. Nevertheless, the explanatory charitable role of free space in the realm of evolutionary game theory has been less explored till now.

This present article considers two different traditional symmetric two-person games: PD and SD. The sole motivation behind the choice of two dissimilar games is to capture the essence of behavioural heterogeneity [55–58] among social creatures. Interaction between subpopulations

of different cultural backgrounds has potential impacts on the cooperation level. There are other two-person games, but these two games have attracted a lot of attention for their simplicity and enormous applications in social, ecological and biological systems [16,27,59–61]. The population of players plays the PD game with probability p, whereas they can play the SD game with complementary probability $(1 - p)$. Additionally, we consider the advantages provided by the free space for all other individuals. Here, free space is treated as an ecological variable that does not expect any benefits for its selfless act. This one-sided altruistic behaviour is omnipresent in our society even though selfish actions by an agent fetch it relatively more benefit. The sharing of resources with people in need, the decent actions of men in the presence of an attractive woman and holding the door open for strangers are all well-known examples of altruism. The introduction of this ecological variable helps us to derive an eco-evolutionary model [62–72] that triggers a valuable way of analysing the simultaneous impact of ecological and evolutionary changes. Furthermore, we incorporate the influence of punishment on evolutionary dynamics, which often arises spontaneously as a way of penalizing the defectors for their free-riding mentality. Most of the previous studies on punishment deal with public goods games [73–76] and the impact of punishment on evolutionary multi-game [77–79] has yet to gain its well-deserved attention.

The proposed eco-evolutionary theoretical framework gives rise to rich dynamical complexities with several evolutionary stable states. The resulting dynamics might be capable of unfolding new fascinating trends in understanding the interactions of ecological and evolutionary processes. The long-term behaviour of our model under favourable circumstances may lead to periodic dynamics indicating the spontaneous emergence of cyclic dominance [26,80–82]. Several real-life examples, including the mating strategy of side-blotched lizards [83], accidental extinction of one of the participating species [84], fundamental problems of stability for the competition of two defensive alliances [85], an explanation of the oscillating frequency of lemmings [86], the genetic regulation in the repressilator [87] and so on, display such a procedure of cyclical interactions. The probabilistic nature of our model seems more promising for encapsulating biodiversity with slow–fast dynamics [88–90], which is quite common in the atmosphere and oceanic dynamics. The stationary states are interpreted using the game-theoretic concepts of the Nash equilibrium and the evolutionarily stable strategy. The emergence of stationary states on coupled systems [91–97] also attracts numerous researchers of nonlinear dynamics due to their multiple practical applications.

Besides such convergent stationary point outcomes, the dynamics of competing subpopulations also exhibit the non-stationary point complex solutions in the form of chaotic attractors [98–102]. Such a strange chaotic coexistence prevents each subpopulation from becoming extinct. This highly irregular fluctuation portrays the sensitive dependence on initial conditions. In fact, our proposed model is multi-stable, indicating the vulnerability of the system to small perturbations. Unfortunately, this chaotic attractor for chosen parameter values represents an overcrowded solution as the density of each subpopulation lies outside the closed interval $[0, 1]$. In fact, the meaning of chaos, i.e. the coexistence of a countably infinite number of unstable periodic orbits from the contexts of game theory, is not well understood yet. However, still we can provide a comprehensive picture of the overall dynamics through the bifurcation analysis. The reason behind the sudden demolition of attractors for some specific choices of parameters is illustrated through the collision of the chaotic attractor with a coexisting unstable stationary point [103–105]. The subsequent part of this paper is organized as follows. We elaborately discuss our eco-evolutionary model in the presence of cooperators, defectors and punishers under the influence of philanthropic free space in §2. After a detailed description of our model, we describe the dynamics using various bifurcation diagrams in §3. For particular parameter values, we scrutinize the basin of attraction, revealing multi-stable behaviour. The theoretical findings through stability analysis are validated using rigorous numerical studies. We also provide a special case where the free space yields equally likely benefits to each subpopulation. Finally, we summarize our results with some conclusions in §4.

2. Mathematical model

To capture the evolving pattern of real-world systems, we consider two archetypal models of social interaction, *viz.* the PD and SD games. These models can describe the essence of several social puzzles, even though they cannot capture many details of the complex real-life interactions. In these games, two individuals play against each other, and they must choose between two possible actions: cooperation (**C**) and defection (**D**). The joint behaviour of the two players for these two games is represented by the following 2×2 payoff matrix

$$
\begin{array}{cc}
& \begin{array}{cc} \mathbf{C} & \mathbf{D} \end{array} \\
\begin{array}{c} \mathbf{C} \\ \mathbf{D} \end{array} & \begin{pmatrix} R & S \\ T & P \end{pmatrix}.
\end{array}
$$

The payoff value R signifies a reward towards both players choosing **C**. A defector playing with another defector yields the punishment P. The temptation T is given to a defector for exploiting a cooperator. By comparison, the exploited cooperator receives the sucker's payoff S for playing with a defector. Depending upon the ordering of these four payoff values, we may be able to achieve different 2×2 games. If the ranking of these payoffs is $T > R > P > S$, we arrive at the classical PD game. This inequality suggests defection is the best and an intelligent choice for the self-interested individuals regardless of the opponent's strategy. If another partner chooses to cooperate, then the defector gains more as $T > R$. If the other player decides to defect, defection also brings a better payoff as $P > S$. Consequently, both players end up with P, as defection is the dominant strategy for both players. Thus, in any circumstances, the cooperators lead to extinction, unable to resist invasion by defectors. But the payoff relation $R > P$ suggests mutual cooperation is superior in terms of payoff to the dominant strategy mutual defection. This dilemma describes how cooperation arises spontaneously in the evolution of species ranging from single cellular organisms to vertebrates opposing the fact that widespread defection is predicted by game theory. Interestingly, a slight variation in the ordering of these payoff values, such as $T > R > S > P$, leads to a more favourable game for cooperators. Note that only the ranking of P and S is exchanged compared with the PD game. Now, the best action depends on the opponent. Rational players will defect if the other cooperates, but will cooperate if the other defects to maximize their respective payoffs. This game is known as the SD game. Despite the notable difference of both game dynamics, the $R > P$ relation holds in both games, suggesting the interaction between two defectors is worse than the interaction between two cooperators.

We consider an additional strategy punishment (**P**) to impose a fine on defectors for their free-riding behaviour and exploitation of collective efforts. This independent strategy is a special kind of cooperation. Whenever a punisher meets a cooperator, they will both receive the reward R. A defector earns a reduced payoff value of $T - \delta$ when confronted by a punisher. By comparison, a punisher will get $S - \delta$ if the other player decides to defect. This $\delta > 0$ is the amount of fine deducted from a defector's payoff to maintain a better environment for the survival of cooperation. However, the punisher has to put up with the cost of policing $\delta > 0$ too. We also consider free space (**F**) as an ecological variable. Any player can use the free space for their replication, and free space unselfishly reduces its fitness by helping others without any expectations of reward. We incorporate this necessary altruistic behaviour of free space in the payoff matrix by assuming that the free space will receive a payoff value 0 when it interacts with others. Although it provides a positive payoff σ_1, σ_2, and σ_3 to cooperators, punishers and defectors, respectively. Without loss of any generality, the payoff values are taken as $R_{\mathrm{PD}} = R_{\mathrm{SD}} = 1$, $S_{\mathrm{PD}} = S_{\mathrm{SD}} = 0$, $T_{\mathrm{PD}} = T_{\mathrm{SD}} = \beta > 1$, $P_{\mathrm{PD}} = \eta \in [0, 1)$ and $P_{\mathrm{SD}} = -\eta \in (-1, 0]$. Thus, we arrive at two distinct payoff

matrices:

$$A = \begin{array}{c} \\ \text{C} \\ \text{P} \\ \text{D} \\ \text{F} \end{array} \begin{array}{cccc} \text{C} & \text{P} & \text{D} & \text{F} \\ \begin{pmatrix} 1 & 1 & 0 & \sigma_1 \\ 1 & 1 & -\delta & \sigma_2 \\ \beta & \beta - \delta & \eta & \sigma_3 \\ 0 & 0 & 0 & 0 \end{pmatrix} \end{array} \quad \text{and} \quad B = \begin{array}{c} \\ \text{C} \\ \text{P} \\ \text{D} \\ \text{F} \end{array} \begin{array}{cccc} \text{C} & \text{P} & \text{D} & \text{F} \\ \begin{pmatrix} 1 & 1 & 0 & \sigma_1 \\ 1 & 1 & -\delta & \sigma_2 \\ \beta & \beta - \delta & -\eta & \sigma_3 \\ 0 & 0 & 0 & 0 \end{pmatrix} \end{array} \tag{2.1}$$

in which the entries portray the payoff accumulated by the players on the left. A and B are the matrices corresponding to the PD and SD games, respectively. A population of players can play the PD game with probability p, and they can play the SD game with the complementary probability $(1 - p)$. Thus, we obtain a payoff matrix for the two games as

$$E = pA + (1 - p)B = \begin{array}{c} \\ \text{C} \\ \text{P} \\ \text{D} \\ \text{F} \end{array} \begin{array}{cccc} \text{C} & \text{P} & \text{D} & \text{F} \\ \begin{pmatrix} 1 & 1 & 0 & \sigma_1 \\ 1 & 1 & -\delta & \sigma_2 \\ \beta & \beta - \delta & 2p\eta - \eta & \sigma_3 \\ 0 & 0 & 0 & 0 \end{pmatrix} \end{array}. \tag{2.2}$$

Note that if we choose $\eta = 0$ then the term containing both p and η will vanish. Hence, we eliminate the case $\eta = 0$ from our study and choose $\eta \in (0, 1)$, as we wish to investigate the impact of varying p. The payoff values of E are obtained from the interactions of the games. We treat these payoff values as reproductive success. Hence, a player with a higher payoff can leave more offspring. We assume that x, y, z and w are the fractions of cooperators, punishers, defectors and free space, respectively. The combination of game dynamics and ecological dynamics helps us to construct a system of nonlinear equations. The available free space $w = 1 - (x + y + z)$ lies within the closed interval $[0, 1]$. When $w = 0$, then overall population density $x + y + z$ reaches 1. This case ($w = 0$) represents the unavailability of reproductive opportunities. On the other hand, $w = 1$ reflects the extinction of the overall population with $x + y + z = 0$. Let f_C, f_P, f_D and f_F be the average payoffs of cooperators, punishers, defectors and free space, respectively, at any given point of time. These average payoffs can be easily calculated from the payoff matrix E. Clearly,

$$f_F = 0, \tag{2.3}$$

as free space promotes everyone else's welfare without taking any advantage from others. The average payoff of cooperators is given by

$$f_C = x + y + \sigma_1 w = (1 - \sigma_1)x + (1 - \sigma_1)y - \sigma_1 z + \sigma_1. \tag{2.4}$$

Here, we eliminate the variable w using the relation $x + y + z + w = 1$. Similarly, the average payoffs of punishers and defectors are given by

$$f_P = (1 - \sigma_2)x + (1 - \sigma_2)y - (\delta + \sigma_2)z + \sigma_2 \tag{2.5}$$

and

$$f_D = (\beta - \sigma_3)x + (\beta - \delta - \sigma_3)y + (2p\eta - \eta - \sigma_3)z + \sigma_3. \tag{2.6}$$

Thus, the fractions x, y and z can control the average payoffs f_C of cooperators, f_P of punisher and f_D of defectors at any given point in time. We further assume these average payoffs can uniquely determine their respective birth rates, and all individuals die at an equal and constant rate $\xi > 0$. Thus, we obtain a simple eco-evolutionary dynamical model describing the changes in frequencies of cooperators, punishers and defectors over time as follows:

$$\left. \begin{aligned} \dot{x} &= x[f_C - \xi], \\ \dot{y} &= y[f_P - \xi] \\ \dot{z} &= z[f_D - \xi]. \end{aligned} \right\} \tag{2.7}$$

and

Table 1. Parameters with their respective domain and their physical significance.

parameters	physical interpretation	domain
ξ	constant death rate	>0
β	temptation parameter	>1
δ	fine for controlling selfish behaviour of defectors	>0
p	probability of playing PD game	[0, 1]
η	payoff for mutual defection	(0, 1)
σ_1	free space-induced benefit towards C	>0
σ_2	free space-induced benefit towards P	>0
σ_3	free space-induced benefit towards D	>0

One should notice that the *per capita* growth rate of each of the subpopulations **C**, **P** and **D** depends on the fraction of free space w, and the free space-induced benefits σ_1, σ_2 and σ_3. They have a vital role in the fitnesses of all subpopulations. Thus, the inclusion of this effect of free space in the reproduction rate of all subpopulations helps us to exclude the unnecessary multiplication of w with their average payoffs, which is often observed in the previous studies [62,70]. Moreover, along the line of earlier works [62,67,70], this set of equations is a natural extension of the replicator dynamics [15,106].[1]

Since $w = 1 - (x + y + z)$, thus the frequencies of free space change over time using the following relation:

$$\dot{w} = -\dot{x} - \dot{y} - \dot{z}. \tag{2.9}$$

Substituting the expressions of f_C from equation (2.4), f_P from equation (2.5) and f_D from equation (2.6) in equation (2.7), we get the following eco-evolutionary model:

$$\left. \begin{aligned} \dot{x} &= x[(1 - \sigma_1)x + (1 - \sigma_1)y - \sigma_1 z + (\sigma_1 - \xi)], \\ \dot{y} &= y[(1 - \sigma_2)x + (1 - \sigma_2)y - (\sigma_2 + \delta)z + (\sigma_2 - \xi)] \\ \dot{z} &= z[(\beta - \sigma_3)x + (\beta - \delta - \sigma_3)y + (2p\eta - \eta - \sigma_3)z + (\sigma_3 - \xi)], \end{aligned} \right\} \tag{2.10}$$

and

with the parameters $\eta \in (0, 1)$, $p \in [0, 1]$, $\beta > 1$ and δ, ξ, σ_1, σ_2, $\sigma_3 > 0$. The physical interpretation of each parameter is given in table 1.

3. Results

(a) Multi-stability

For the numerical investigation, the system (2.10) is integrated using the Runge–Kutta fourth-order method with integration step-length $h = 0.01$. The simulations are performed for 1.2×10^6 iterations unless stated otherwise. At first, we discuss the role of initial conditions on our proposed model. Since the fractions of each subpopulation must lie within the closed interval [0, 1] for physically meaningful solutions in the context of evolutionary game theory, we only choose initial conditions (x_0, y_0, z_0) maintaining the constraint $x_0 + y_0 + z_0 + w_0 = 1$. In figure 1 for a specific choice of parametric values, we choose four different initial conditions for which the trajectories of system (2.10) converge to diverse attractors. Throughout the article, we maintain the relation $x_0 + y_0 + z_0 = 0.9$ unless stated otherwise. The existence of solutions of the system (2.10) is

---

[1]The extraction of traditional replicator dynamics is possible by using $\xi = \bar{f}$, where

$$\bar{f} = \frac{xf_C + yf_P + zf_D}{x + y + z} = \frac{xf_C + yf_P + zf_D}{1 - w} \tag{2.8}$$
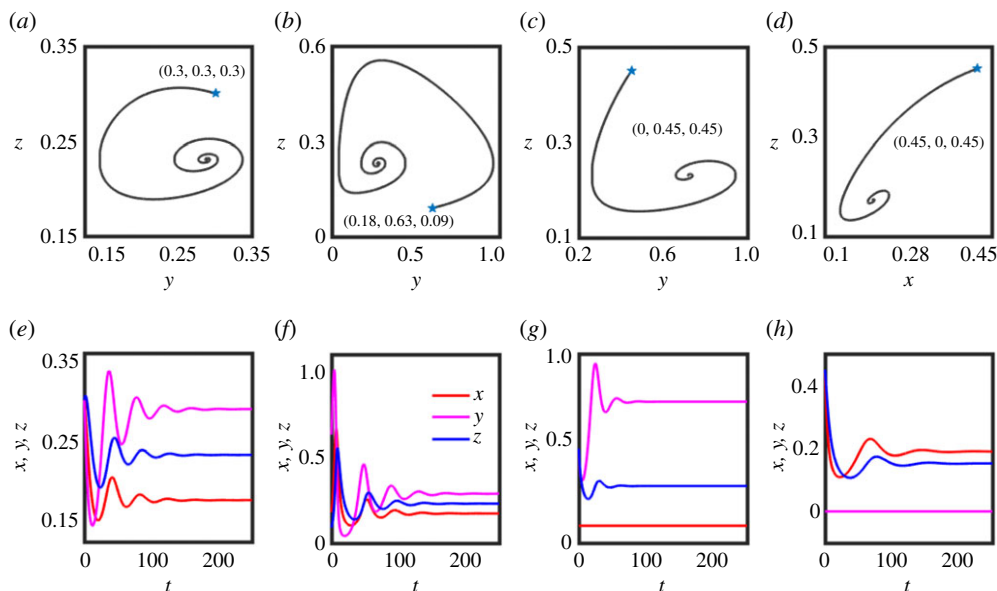
indicates the mean fitness with $w \neq 1$.

Figure 1. (a–h) Multi-stability: We use four distinct initial conditions to understand the multi-stable behaviour of the proposed model (2.10). Each column represents the same attractor, where the top panel depicts the two-dimensional projection of the attractor, and the bottom panel portrays the temporal evolution of the three subpopulations. The pentagram marker indicates the initial condition, which is also explicitly written in each subfigure. Red, magenta and blue regions designate the fraction of cooperators x, punishers y and defectors z, respectively. The interior initial condition ($x_0 \neq 0$, $y_0 \neq 0$, $z_0 \neq 0$) always gives rise to the interior stationary point E_7. The initial condition with at least one zero component leads to other solutions. For other information, see the text. Parameters: $\sigma_1 = 0.775$, $\sigma_2 = 1.0$, $\sigma_3 = 0.7$, $\beta = 1.2$, $\delta = 0.3$, $\xi = 0.7$, $p = 0.55$ and $\eta = 0.75$. (Online version in colour.)

assured since the right-hand side of each of the nonlinear equations is continuously differentiable. In fact, the right-hand side of the system (2.10) is locally Lipschitz for any bounded subset of $\mathbb{R}^+ \cup \{0\} \times \mathbb{R}^+ \cup \{0\} \times \mathbb{R}^+ \cup \{0\}$. Hence for any non-negative initial condition, the uniqueness of the solution of the system (2.10) is guaranteed.

The solution corresponding to the initial condition $(0.45, 0.45, 0)$ leads to an unbounded solution. This result is not shown in figure 1. However, a different cooperator-free solution appears for the initial condition $(0, 0.45, 0.45)$, as shown in figure 1c,g. This result is physically meaningful, as initially there is no subpopulation of cooperators ($x_0 = 0$), so there is no chance of reproducing **C** in the future. Additionally, a close inspection of the right-hand sides of the equations (2.10) suggests that $(0, 0, 0)$ is a stationary point of the system.

We denote the stationary point $(0, 0, 0)$ as E_0. A different initial condition $(0.45, 0, 0.45)$ for the same set of parameter values brings the punisher-free solution (figure 1d,h). One may be surprised that the initial condition $(0.45, 0.45, 0)$ does not help reach the defector-free stationary point $E_4 = (\alpha_1, \alpha_2, 0)$ with $0 < \alpha_1 + \alpha_2 = (\xi - \sigma_1)/(1 - \sigma_1) = (\xi - \sigma_2)/(1 - \sigma_2) \leq 1$. This is due to our choice of parameter values in figure 1. The stationary point E_4 exists if $\xi = 1$ or $\sigma_1 = \sigma_2$. Moreover, its stability depends on the following eigenvalues

$$
\begin{cases}
\lambda_1 = \sigma_3 - \xi + (\beta - \sigma_3)(\alpha_1 + \alpha_2) - \delta\alpha_2, \\
\text{and the two roots of the equation} \\
\lambda^2 - \lambda[\sigma_1 + \sigma_2 - 2\xi - 2\alpha_1(\sigma_1 - 1) - \alpha_2(\sigma_1 - 1) - \alpha_1(\sigma_2 - 1) - 2\alpha_2(\sigma_2 - 1)] \\
\quad -\alpha_1\alpha_2(\sigma_1 - 1)(\sigma_2 - 1) = 0.
\end{cases}
\tag{3.1}
$$

Interestingly in figure 1d,h, the fraction of cooperation dominates the fraction of defectors as $x > z$, although initially we choose $x_0 = z_0 = 0.45$. In fact, the initial conditions in figure 1a,b,c,e,f,g

are found to be effective for forming punisher clusters. In all these figures, the relation $y > z > x$ indicates the increment of the degree of punishers in a significant way. For figure 1*a,b* and *e,f*, the trajectories converge to the interior stationary point $E_7 = (x^*, y^*, z^*)$ for two non-identical initial conditions $(0.3, 0.3, 0.3)$ and $(0.18, 0.63, 0.09)$. Here,

$$
\begin{aligned}
x^* &= \frac{\Delta_2}{\delta(\delta - \sigma_1 + \sigma_2 - \delta\sigma_1)}, \\
\Delta_2 &= \eta\sigma_2 - \eta\sigma_1 - \delta\sigma_3 + \delta\xi - \sigma_1\xi + \sigma_2\xi - \delta^2\sigma_1 + \delta^2\xi + \beta\delta\sigma_1 \\
&\quad - \beta\delta\xi + 2\eta p\sigma_1 - 2\eta p\sigma_2 + \beta\sigma_1\xi - \beta\sigma_2\xi - 2\delta\sigma_1\xi \\
&\quad + \delta\sigma_2\xi + \delta\sigma_3\xi + \eta\sigma_1\xi - \eta\sigma_2\xi - 2\eta p\sigma_1\xi + 2\eta p\sigma_2\xi, \\
y^* &= \frac{\Delta_3}{\delta(\delta - \sigma_1 + \sigma_2 - \delta\sigma_1)}, \\
\Delta_3 &= \delta\sigma_3 + \eta\sigma_1 - \eta\sigma_2 - \delta\xi + \sigma_1\xi - \sigma_2\xi - \beta\delta\sigma_1 + \beta\delta\xi - 2\eta p\sigma_1 + 2\eta p\sigma_2 \\
&\quad - \beta\sigma_1\xi + \beta\sigma_2\xi + \delta\sigma_1\xi - \delta\sigma_3\xi - \eta\sigma_1\xi + \eta\sigma_2\xi + 2\eta p\sigma_1\xi - 2\eta p\sigma_2\xi
\end{aligned}
$$

and

$$
z^* = \frac{\sigma_2 - \sigma_1 + \sigma_1\xi - \sigma_2\xi}{\delta - \sigma_1 + \sigma_2 - \delta\sigma_1}. \tag{3.2}
$$

For a physically meaningful solution, the constraints $x^*, y^*, z^* \in (0, 1)$ and $x^* + y^* + z^* \in (0, 1]$ are maintained. The solution transforms to $E_7 = (x^*, y^*, z^*) = (0.1731, 0.2885, 0.2308)$ for the set of parameters $\sigma_1 = 0.775$, $\sigma_2 = 1.0$, $\sigma_3 = 0.7$, $\beta = 1.2$, $\delta = 0.3$, $\xi = 0.7$, $p = 0.55$ and $\eta = 0.75$ used in figure 1. Figure 1*a,e* reveals how this set of parameters tends to favour punishers, although initially, the fractions of all subpopulations are equally distributed with $x_0 = y_0 = z_0 = 0.3$ and $x_0 + y_0 + z_0 = 0.9$. Besides, we choose a different interior initial point $(0.18, 0.63, 0.09)$. For this initial condition too, the system (2.10) converges to the interior equilibrium point E_7 (figure 1*b,f*). Although here $x_0 = 2z_0$ and $y_0 = 7z_0$, the defectors are not outperformed by cooperators in the long-term asymptotic behaviour. This scenario helps to sustain the punishers to resist the invasion of defectors. The collective behaviour of figure 1 may suggest that the multi-stability of our eco-evolutionary model occurs only at the boundary of the basin of attraction with at least one zero component. But there still are a few suitable choices of parameters enabling the multi-stable behaviour of the system with interior initial conditions. Figure 2 delineates the basin of attraction for the set of parameters $\sigma_1 = 1.2$, $\sigma_2 = 1.5$, $\sigma_3 = 1.4$, $\beta = 1.5$, $\delta = 0.5$, $\xi = 1.1$, $\eta = 0.1$ and $p = 0.1$. This set of parameters satisfies the stability criterion of both the stationary points $E_2 = (0, (\xi - \sigma_2)/(1 - \sigma_2), 0)$ with $0 < (\xi - \sigma_2)/(1 - \sigma_2) \le 1$ and $E_3 = (0, 0, (\xi - \sigma_3)/(2p\eta - \sigma_3 - \eta))$ with $0 < (\xi - \sigma_3)/(2p\eta - \sigma_3 - \eta) \le 1$. The eigenvalues of the Jacobian matrix corresponding to the stationary point E_2 are

$$
\begin{aligned}
\lambda_1 &= \xi - \sigma_2, \\
\lambda_2 &= -\frac{\sigma_3 - \xi - \beta\sigma_2 + \delta\sigma_2 + \beta\xi - \delta\xi + \sigma_2\xi - \sigma_3\xi}{\sigma_2 - 1}
\end{aligned}
$$

and

$$
\lambda_3 = -\frac{\sigma_1 - \sigma_2 - \sigma_1\xi + \sigma_2\xi}{\sigma_2 - 1}. \tag{3.3}
$$

The eigenvalues of the Jacobian matrix corresponding to the stationary point E_3 are

$$
\begin{aligned}
\lambda_1 &= \xi - \sigma_3, \\
\lambda_2 &= \sigma_2 - \xi - \frac{(\delta + \sigma_2)(\sigma_3 - \xi)}{\eta + \sigma_3 - 2p\eta}
\end{aligned}
$$

and

$$
\lambda_3 = \sigma_1 - \xi - \frac{\sigma_1(\sigma_3 - \xi)}{\eta + \sigma_3 - 2p\eta}. \tag{3.4}
$$

We perform the numerical investigation in figure 2 maintaining the relation $x_0 + y_0 + z_0 = 0.9$ as mentioned earlier. Such a constraint allows considering an initial point $(0.9, 0, 0)$. This type of
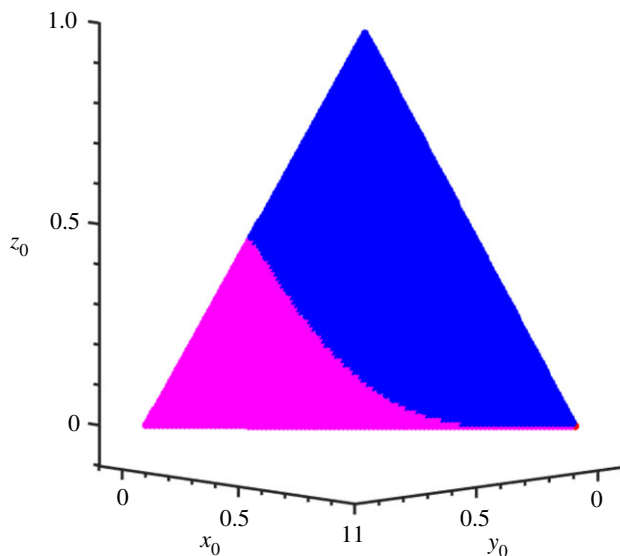
Figure 2. Basin of attraction: Red, magenta and blue regions represent the three distinct stationary points E_1, E_2 and E_3, respectively. The simulations are performed for sufficiently long iterations (1.5×10^7). Initial conditions are varied by preserving the constraint $x_0 + y_0 + z_0 = 0.9$. Only the initial condition $(0.9, 0, 0)$ tends to the punisher-free and defector-free stationary point E_1. Other initial conditions cause a cooperator-free society. Depending on those initial conditions, the system facilitates either the promotion of defectors or the emergence of punishers. Parameters: $\sigma_1 = 1.2, \sigma_2 = 1.5, \sigma_3 = 1.4, \beta = 1.5, \delta = 0.5$, $\xi = 1.1, \eta = 0.1$ and $p = 0.1$. The coexistence of these different stable states reveals the manifestation of multi-stability in our proposed model. For further details, go through the main text. (Online version in colour.)

initial condition with $y_0 = 0$ and $z_0 = 0$ allows the system (2.10) to converge to the stationary state $E_1 = ((\xi - \sigma_1)/(1 - \sigma_1), 0, 0)$ with $0 < (\xi - \sigma_1)/(1 - \sigma_1) \leq 1$. The eigenvalues of the Jacobian matrix corresponding to the stationary point E_1 are

$$\left. \begin{aligned} \lambda_1 &= \xi - \sigma_1, \\ \lambda_2 &= \sigma_3 - \xi + \frac{(\beta - \sigma_3)(\sigma_1 - \xi)}{\sigma_1 - 1} \\ \lambda_3 &= \sigma_2 - \xi - \frac{(\sigma_2 - 1)(\sigma_1 - \xi)}{\sigma_1 - 1}. \end{aligned} \right\} \tag{3.5}$$

and

In fact, our proposed model with $(x_0, 0, 0)$ initial condition $(x_0 \neq 0)$ gives rise to the solution

$$x = \frac{(\sigma_1 - \xi)\left(1 + \tanh\left(c_1 + t\right)\left((\sigma_1/2) - (\xi/2)\right)\right)}{2\sigma_1 - 2}, y = 0 \text{ and } z = 0, \tag{3.6}$$

where c_1 is the initial condition-dependent constant. Similarly, the initial condition $(0, y_0, 0)$ with $y_0 \neq 0$ leads to the solution

$$x = 0, \quad y = \frac{(\sigma_2 - \xi)\left(1 + \tanh\left(c_2 + t\right)\left((\sigma_2/2) - (\xi/2)\right)\right)}{2\sigma_2 - 2} \text{ and } z = 0, \tag{3.7}$$

and the initial condition $(0, 0, z_0)$ with $z_0 \neq 0$ brings

$$x = 0, \quad y = 0 \text{ and } z = \frac{(\sigma_3 - \xi)\left(1 + \tanh\left(c_3 + t\right)\left((\sigma_3/2) - (\xi/2)\right)\right)}{2\eta + 2\sigma_3 - 4\eta p}, \tag{3.8}$$

where c_2 and c_3 are the initial condition-dependent constants. The multi-stable behaviour of our model is depicted through figure 2, where red, magenta and blue signify the convergence

towards the stationary points E_1, E_2 and E_3, respectively. This universal nonlinear aspect of multi-stability plays the role of a pivot towards the emergence and switching among several stable states [96,107,108]. Thus, to neglect the multi-stability of the eco-evolutionary dynamics, we fix the initial condition $(0.3, 0.3, 0.3)$ throughout the rest of the article. This choice does not provide any biased attitude towards any subpopulations, as we choose an equal initial value $x_0 = y_0 = z_0 = 0.3$. We also maintain the constraint $x_0 + y_0 + z_0 = 0.9$ for this specific choice.

(b) Interplay of different parameters

Now, we investigate the role of parameters on our proposed model. Figure 3*a* describes the impact of the temptation parameter $\beta \in (1, 2)$. The increment of β provides additional benefits to defectors. Thus, beyond a certain threshold of β, the invasion of defectors challenges the sustainability of cooperators. The cooperators survive within the range $(1, 1.31]$. Here, the stationary point E_7 describes the coexistence of all subpopulations. Although the fraction of cooperators show a decreasing trend within $\beta \in (1, 1.31]$, however it promotes the punisher's population y. y increases initially till $\beta \approx 1.31$. After that it experiences a reduction along with the extinction of cooperators. But a natural expectation of growth in the defector's population is not observed in this figure. z remains constant throughout the interval $\beta \in (1, 2)$ for our choice of parameters $\sigma_1 = 0.775$, $\sigma_2 = 1.0$, $\sigma_3 = 0.7$, $\delta = 0.3$, $\xi = 0.7$, $p = 0.55$ and $\eta = 0.75$. The interplay between other parameters may restrict the increment of z. For the chosen set of parameters, the stationary point $E_5 = (0, \beta_1, \beta_2)$ stabilizes for $\beta > 1.31$. Here,

$$
\left.
\begin{aligned}
\beta_1 &= \frac{\delta\sigma_3 - \eta\sigma_2 - \delta\xi + \eta\xi - \sigma_2\xi + \sigma_3\xi + 2p\eta\sigma_2 - 2p\eta\xi}{\eta + \sigma_3 - \beta\delta - \sigma_2\beta - 2p\eta + \delta\sigma_2 + \delta\sigma_3 - \eta\sigma_2 + \delta^2 + 2p\eta\sigma_2} \\
\text{and} \quad \beta_2 &= \frac{\sigma_3 - \xi - \beta\sigma_2 + \delta\sigma_2 + \beta\xi - \delta\xi + \sigma_2\xi - \sigma_3\xi}{\eta + \sigma_3 - \beta\delta - \sigma_2\beta - 2p\eta + \delta\sigma_2 + \delta\sigma_3 - \eta\sigma_2 + \delta^2 + 2p\eta\sigma_2}
\end{aligned}
\right\}
\tag{3.9}
$$

with β_1, $\beta_2 \in (0, 1)$ and $\beta_1 + \beta_2 \in (0, 1]$.

The coexistence of punishers and defectors is found to occur also in $\delta \in (0, 0.115)$, as shown in figure 3*b*. Other parameters are set at the same values, just like in figure 3*a* with $\beta = 1.1$. The emergence of cooperation along with punishers and defectors is noticed in $\delta \in [0.115, 0.7]$. The fraction of defectors shows a decreasing tendency till $\delta = 0.7$, after which the value of z saturates. This declination of defector's frequency allows the cooperators to thrive. However, the uprise of δ harms the punishers. Initially, the subpopulation of **P** enjoys dominance over the defectors and exhibits a monotonic increasing behaviour till $\delta = (0, 0.115)$. For $\delta \geq 0.115$, the fraction of punishers y experiences a monotonically drop off, and ultimately it will dwindle to zero at $\delta = 0.7$. This behaviour of y is mainly due to the nature of punishers who always impose a fine δ on defectors. Besides, the punishers have to bear the same amount of cost from its payoff. Thus, the increment of δ leads to an unfavourable scenario for the punishers. However, the existence of punishers constantly challenges the defectors. Thus, the density of defectors decreases with the presence of punishers. As soon as punishers die out, the fraction of defectors saturates. For $\delta > 0.21$, cooperation emerges as the dominant strategy over other subpopulations. At $\delta = 0.7$, the system stabilizes to the punisher-free stationary point $E_6 = (\gamma_1, 0, \gamma_2)$ with $\gamma_1, \gamma_2 \in (0, 1)$ and $\gamma_1 + \gamma_2 \in (0, 1]$. Here,

$$
\left.
\begin{aligned}
\gamma_1 &= -\frac{\eta\sigma_1 - \eta\xi + \sigma_1\xi - \sigma_3\xi - 2p\eta\sigma_1 + 2p\eta\xi}{\eta + \sigma_3 - \beta\sigma_1 - 2p\eta - \eta\sigma_1 + 2p\eta\sigma_1} \\
\text{and} \quad \gamma_2 &= \frac{\sigma_3 - \xi - \beta\sigma_1 + \beta\xi + \sigma_1\xi - \sigma_3\xi}{\eta + \sigma_3 - \beta\sigma_1 - 2p\eta - \eta\sigma_1 + 2p\eta\sigma_1}.
\end{aligned}
\right\}
\tag{3.10}
$$

To realize the role of $\eta \in (0, 1)$, similarly we draw the bifurcation diagram of the population model (2.10) with respect to η in figure 3*c* for fixed parameter values $\sigma_1 = 0.775$, $\sigma_2 = 1.0$, $\sigma_3 = 0.7$, $\beta = 1.1$, $\delta = 0.3$, $\xi = 0.7$ and $p = 0.55$. Clearly, the behaviour of the system remains unaltered as the
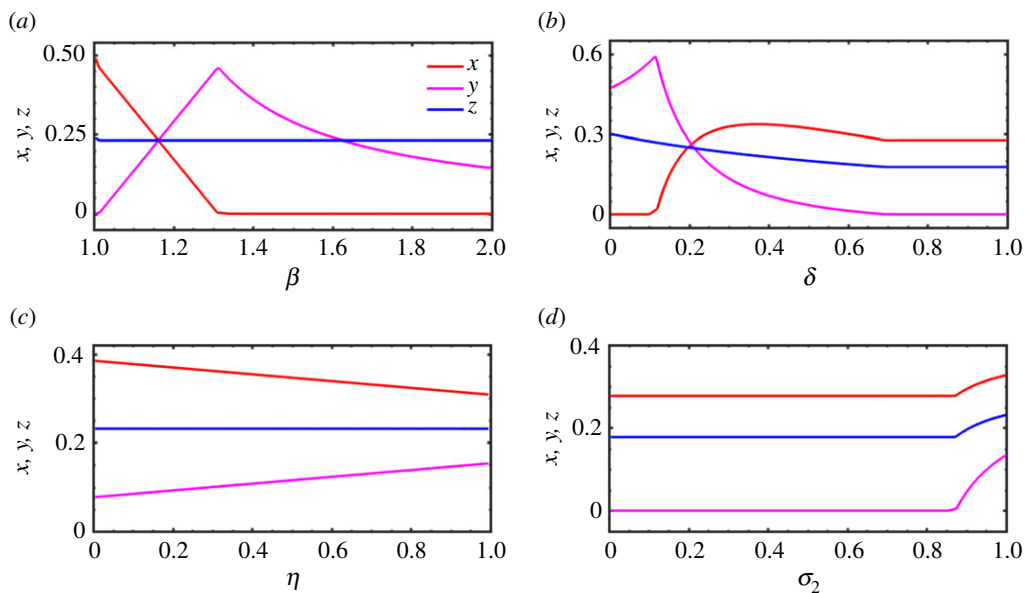
Figure 3. Dependence of different parameters on cooperation, punishment and defection: (*a*) The fraction of cooperators is dramatically decreasing as a function of β. The defectors are getting an additional advantage with increasing β, which causes the extinguishing of cooperators beyond a critical value of β. Punishers are initially enjoying inevitable growth but ultimately strive to survive. Beyond a specific critical value of β, the favourable environment towards defectors increases the likelihood of dominance of D. Here, $\delta = 0.3$, $\eta = 0.75$ and $\sigma_2 = 1.0$. (*b*) A transition from a cooperator-free society to the coexistence of all subpopulations is observed with variation of δ, and ultimately it will originate a punisher-free community at $\delta \approx 0.7$. The punishing cost allows decreasing the rate of defectors. Since the punisher has to tolerate the same burden of punishing, their population will decline to extinction beyond a critical value of δ. Cooperators succeed in dominating the whole population beyond a particular value of δ. Here, $\beta = 1.1$, $\eta = 0.75$ and $\sigma_2 = 1.0$. (*c*) η is never able to destabilize the coexistence of three subpopulations for the choice of parameters $\beta = 1.1$, $\delta = 0.3$ and $\sigma_2 = 1.0$. Yet, as $\eta \to 1-$, the fraction of cooperators decreases, and the fraction of punishers increases. Throughout the interval, cooperation emerges as the dominant strategy. (*d*) Punishers prevail with increment of σ_2 for $\beta = 1.1$, $\delta = 0.3$ and $\eta = 0.75$. Initially, the system (2.10) settles down to the punisher-free stationary point E_6. The free space-induced benefits towards P have a positive effect on the emergence of punishers leading to the coexistence of different subpopulations. Moreover, the enhancement in the subpopulation of punishers is comparatively larger than in the other's subpopulation within the interval $\sigma_2 \in [0.87, 1]$. The red, magenta and blue regions represent the fraction of cooperators x, the fraction of punishers y and the fraction of defectors z. The other parameters are kept fixed at $\sigma_1 = 0.775$, $\sigma_3 = 0.7$, $\xi = 0.7$ and $p = 0.55$. The initial condition is (0.3, 0.3, 0.3) for all subfigures. (Online version in colour.)

observed dynamics $x > z > y$ remains the same throughout the interval $\eta \in (0, 1)$ for our chosen parameter values and fixed initial condition (0.3, 0.3, 0.3). Despite the dominance of cooperators, one may notice that as $\eta \to 1-$, the fraction of cooperators monotonically diminishes. Since mutual defection in our model leads to $(2p\eta - \eta)$, this will reduce to 0.1η for our choice of $p = 0.55$. Thus, this additional incentive towards defectors with increasing η causes a lessening of the fraction of cooperation. At the same time, increasing η helps the evolution of punishers as its fraction y undergoes a monotonic growth. The fraction of defectors remains the same throughout the investigated interval. This finding suggests that the reduction in x yields a positive growth in y. Later, we will show the fascinating emergent dynamics of the proposed system with respect to η for a different set of parameter values in figure 7. There, we will again focus on the role of η with a comprehensive and rigorous analysis and comparative discussion.

In figure 3*d*, we inspect the influence of $\sigma_2 \in (0, 1]$. Cooperation is favoured over the whole interval of $\sigma_2 \in (0, 1]$ for our choice of parameter values and initial condition. The numerical
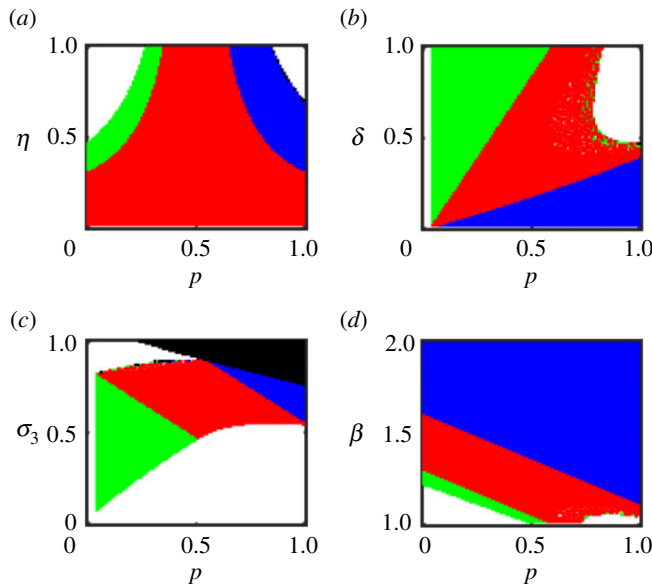
Figure 4. Two parameter phase diagrams of the model with cooperators, punishers and defectors: the increment in p allows everyone to play the PD game more frequently, which in turn inhibits the evolution of cooperation. (*a*) η denotes the mutual defection parameter. For smaller values of p, a suitable range of η facilitates a punisher-free society. Whereas for larger values of p, cooperators cannot resist the invasion of defectors due to the simultaneous impact of both parameters η and p. Finally, C is extinguished, giving rise to the stationary point E_5. Parameters: $\sigma_3 = 0.7$, $\beta = 1.2$ and $\delta = 0.3$. (*b*) For a more significant value of p (transition from blue to red region), the fine δ for restricting the defectors for their selfish mentality is found to be beneficial for the emergence of cooperation. However, the choice of different parameter values also plays an influential role in the proposed model. The additional burden for policing the defectors in terms of higher δ may lead to a punisher-free (green) community. Parameters: $\sigma_3 = 0.7$, $\beta = 1.2$ and $\eta = 0.5$. (*c*) The free space-induced benefits towards defectors offer them a better chance to survive. As a matter of fact, defection is the only possible asymptotic state (black region) for higher values of σ_3 and p. Parameters: $\beta = 1.2$, $\delta = 0.3$ and $\eta = 0.5$. (*d*) Larger β also seems to be unfavourable for cooperators. Parameters: $\sigma_3 = 0.7$, $\delta = 0.3$ and $\eta = 0.5$. Blue, green, red, black and white regions stand for the stationary point E_5, E_6, E_7, E_3 and an overcrowded solution, respectively. Results are obtained for $\sigma_1 = 0.775$, $\sigma_2 = 1.0$ and $\xi = 0.7$. All simulations are done by varying $p \in [0,1]$ for large integrations (1.5×10^7) with fixed initial condition (0.3, 0.3, 0.3). (Online version in colour.)

investigation suggests that the overall dynamics $x > z > y$ remains the same. Yet we anticipate the rise in the subpopulation of the punishers due to the increment of free space-induced benefits towards **P**. But we cannot ignore the role of other parameters. Initially, the system converges to the punisher-free stationary point E_6. At $\sigma_2 \approx 0.87$, the larger social security from the free space gives the punishers opportunity for emergence. The stabilization of the stationary point E_7 allows the survival and coexistence of all subpopulations. In fact within this interval $\sigma_2 \in [0.87, 1]$, the increment of y is slightly better than the other two variables x and z. This signature attests to the positive role of σ_2 over the punishers. Although it never destroys the dominance of cooperators over the other subpopulations, at least for our chosen parameter values and fixed initial condition.

The third row of the payoff matrix (2.2) contains five distinct parameters β, δ, σ_3, p and η. We want to explore the interplay between these parameters. Here, p represents the probability of playing the PD game, where mutual defection is the only strong Nash equilibrium. Definitely, we expect with increasing p, the fraction of cooperation will reduce. This expected behaviour is portrayed through the numerical investigation in figure 4. Figure 4 is drawn for the parameters $\sigma_1 = 0.775$, $\sigma_2 = 1.0$ and $\xi = 0.7$. The simulations are carried out for 1.5×10^7 iterations with fixed initial condition (0.3, 0.3, 0.3). Two-dimensional parameter space with respect to the parameters p and η in figure 4*a* illustrates that the cooperators vanish beyond a critical p. Green, red, blue

and black regions delineate the stationary points E_6, E_7, E_5 and E_3, respectively. The white region describes an overcrowded population with $x + y + z > 1$. However, this regime may contain two different kinds of solutions. An overcrowded solution may represent a solution with $x + y + z > 1$, where each of x, y and z is a finite number. This type of solution is found in the left white portion of figure 4a. There is another possibility of attaining an unbounded solution in terms of x, y and z. This kind of unbounded solution is already observed for $\sigma_1 = 0.775$, $\sigma_2 = 1.0$, $\sigma_3 = 0.7$, $\beta = 1.2$, $\delta = 0.3$, $\xi = 0.7$, $p = 0.55$ and $\eta = 0.75$ (not shown in figure 1) with initial condition $(0.45, 0.45, 0)$. We also detect such an unbounded solution of system (2.10) in the right white portion of figure 4a. Since both solutions are physically meaningless from the context of the game in our study, we do not distinguish between them based on this finiteness and represent them with the same white region.

The transition from E_6 to E_5 via the stabilization of E_7 suggests the enhancement of probability of playing the PD game reduces the chance of survivability of **C**. For smaller values of p, we notice a transition of E_7 (red) to E_6 (green) for increasing η. Since larger values of η indicate a better payoff for mutual defection, it gives rise to a punisher-free society. Smaller values of p bring the further opportunity of playing the SD game where the persistence of cooperation is the expected outcome. A similar kind of transition is noticed from E_7 (red) to E_5 (blue) for increasing η. Here, the extinction of cooperators is encountered for our chosen parametric values. For larger p, individuals get more chance to play the PD game, where defection is the evolutionarily stable strategy, even though all individuals would be better off if they all chose cooperation.

We scrutinize the simultaneous effect of p and δ in figure 4b. This figure reveals that for a suitable intermediate choice of p, increasing δ helps the cooperators to survive, and we observe a transition from E_5 (blue) to E_7 (red). This result displays how punishment towards defectors proves to be effective for the emergence of cooperation. Thus, a cooperator-free community changes the coexistence of all strategies. However, for a smaller value of p, we detect a large region of punisher-free stationary point E_6. Although the cooperators survive against the invading defectors, the punishers must bear a higher policing cost with increasing δ. Thus, this increasing δ provides a less favourable environment for the punishers. Nevertheless, the interplay of other parameters is crucial, proven for a higher value of p. For higher values of p, the system transforms from a cooperator-free society (E_5) to stable coexistence of all subpopulations (E_7), restricting the extinction of punishers.

Figure 4c uncovers the transition from E_6 to E_5 through the stabilization of E_7 in the p-σ_3 plane. The punishers are initially not present in the two-dimensional p-σ_3 plane when the stationary point E_6 only exists. Later, with increasing p, individuals get sufficient opportunity to play both games. This chance of playing the multi-game leads to the survivability of punishers through the coexistence of all subpopulations. Ultimately, the fraction of cooperators asymptotically vanishes in the blue region, as the increment of probability p allows them to play the PD game more, and defectors are fitter in the PD game. Even for a larger value of p and σ_3, we only locate a cooperator-free and punisher-free stationary point E_3 (black). Larger σ_3 generally increases the fitness of defectors, and for $p \to 1-$, individuals play the PD game more often. We all know that defectors are most suited in such circumstances, and hence defectors outcompete other strategies.

For the set of parameter values $\sigma_1 = 0.775$, $\sigma_2 = 1.0$, $\sigma_3 = 0.7$, $\delta = 0.3$, $\xi = 0.7$ and $\eta = 0.5$, we investigate the role of β in figure 4d. With increasing β, the frequency of cooperators should decrease as the advantage of defectors increases. The transition from the stationary point E_6 to E_7 and then the stabilization of E_5 reveals the same story. Initially, the punishers face challenges for survival due to our choice of parameter values and initial conditions. Later, the revival of punishers brings them into the hunt, and the coexistence of all subpopulations occurs. Finally, the cooperators are extinct due to the massive advantage given towards the defectors in terms of temptation parameter β. Now, looking at figure 4d, one can also interpret the positive role of p in our model. Even for moderate smaller values of β, larger p challenges the evolution of cooperation as we obtain the cooperator-free stationary point E_5 (blue). This result is physically meaningful, too, as for larger p, individuals have more tendency to play the PD game. In fact, for larger β, any p does not bring any significant change in the overall dynamics. All the subfigures in

figure 4 contain a white region containing an overcrowded solution. Although they may possess significance from the perspective of nonlinear dynamics, they are physically meaningless as per the game's theoretical aspect. Later, we provide a brief overview of this overcrowded solution using the nonlinear dynamical system approach.

(c) Cyclic dominance

Till now, we are partial towards the stationary point solution of the model (2.10) because it is easier to interpret those results under the limelight of the evolutionary game theory. We have performed a detailed numerical simulation to find a suitable set of parameter values where the existing stationary points are always unstable. We set the parameters at $\sigma_1 = 0.52$, $\sigma_2 = 0.72$, $\sigma_3 = 0.41$, $\beta = 2.60$, $\delta = 1.39$, $\xi = 0.5$, $p = 0.4$ and $\eta = 0.1$. For this set of parametric values, there exist four different biologically significant stationary points $E_0 = (0, 0, 0)$, $E_5 = (0, 0.1815, 0.1283)$, $E_6 = (0.0594, 0, 0.0933)$ and $E_7 = (0.0525, 0.0308, 0.1153)$. There exist other stationary points too, but those stationary points contain negative coordinates. Hence, we do not consider those physically meaningless points in the study. The eigenvalues of the Jacobian corresponding to the extinction stationary point E_0 are

$$
\left.
\begin{aligned}
\lambda_1 &= \sigma_1 - \xi = 0.02, \\
\lambda_2 &= \sigma_2 - \xi = 0.22 \\
\lambda_3 &= \sigma_3 - \xi = -0.09.
\end{aligned}
\right\}
\tag{3.11}
$$

and

The eigenvalues of the Jacobian corresponding to the cooperator-free stationary point E_5 are

$$
\left.
\begin{aligned}
\lambda_1 &= 0.0404, \\
\lambda_2 &= -0.0022 + 0.1911i \\
\lambda_3 &= -0.0022 - 0.1911i.
\end{aligned}
\right\}
\tag{3.12}
$$

and

The eigenvalues of the Jacobian corresponding to the punisher-free stationary point E_6 are

$$
\left.
\begin{aligned}
\lambda_1 &= 0.0398, \\
\lambda_2 &= -0.0058 + 0.0717i \\
\lambda_3 &= -0.0058 - 0.0717i.
\end{aligned}
\right\}
\tag{3.13}
$$

and

The eigenvalues of the Jacobian corresponding to the interior stationary point E_7 are

$$
\left.
\begin{aligned}
\lambda_1 &= -0.0199, \\
\lambda_2 &= 0.0021 + 0.1062i \\
\lambda_3 &= 0.0021 - 0.1062i.
\end{aligned}
\right\}
\tag{3.14}
$$

and

Thus, E_0 is a saddle, whereas the other stationary points E_5, E_6 and E_7 are saddle-foci. All these suggest the trajectories will not settle down to a constant vector. The solution of the system (2.10) must be a function of time wandering in the orthant $\mathbb{R}^+ \times \mathbb{R}^+ \times \mathbb{R}^+$. If the solution is a bounded vector exhibiting periodic behaviour, then the system possesses a limit cycle. We observe the emergent eco-evolutionary dynamics after running for sufficiently long iterations (1.5×10^7) to avoid computational error due to sensitive initial data. The system exhibits a periodic attractor for this set of parameter values (figure 5). The two-dimensional phase space projections in figure 5*f*–*h* suggest the saddle-focus E_7 (shown by hexagram marker) always lies within the interior of the closed trajectory. Figure 5 reveals another interesting dynamical feature of this periodic attractor. For this set of parametric values and fixed initial condition $(0.3, 0.3, 0.3)$, the
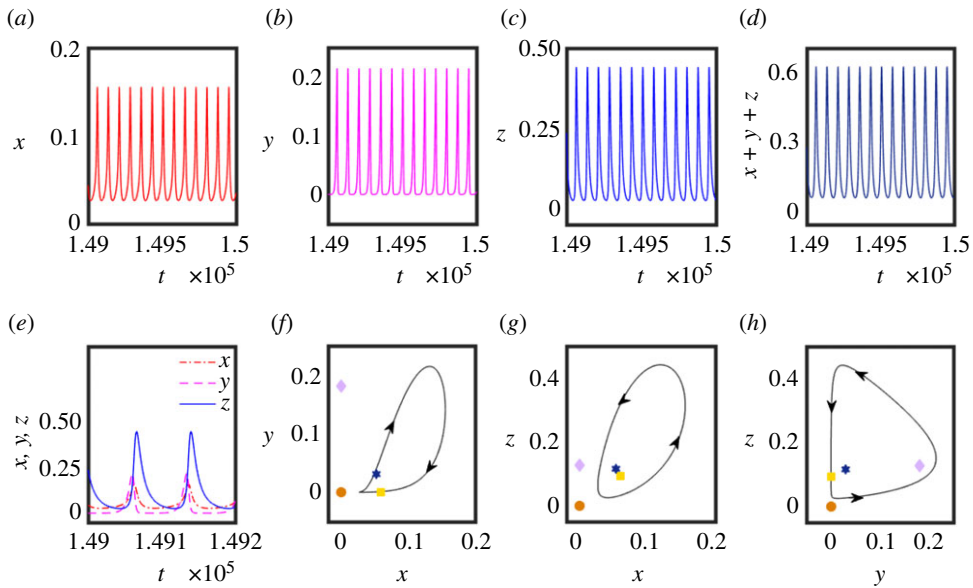
Figure 5. Time evolution of strategies: the periodic dynamics indicate a loop of cyclic dominance, allowing the maintenance of biodiversity through the coexistence of three strategies. The evolutionary dynamics help maintain a degree of cooperation, even under the adverse condition with such an enormous temptation to defect. Individual dynamics of each subpopulation is shown in subfigures (*a–c*). The overall population density is reflected through the subfigure (*d*). Parameters are set at $\sigma_1 = 0.52, \sigma_2 = 0.72, \sigma_3 = 0.41, \beta = 2.60, \delta = 1.39, \xi = 0.5, p = 0.4$ and $\eta = 0.1$. The simulations are carried out for 1.5×10^7 iterations with fixed integration time-step $h = 0.01$. The oscillatory dynamics of x, y and z in subfigure (*e*) allow all cyclically competing strategies to coexist. The extinction saddle E_0, the cooperator-free saddle-focus E_5, the punisher-free saddle-focus E_6 and the interior saddle-focus E_7 are shown by circle, diamond, square and hexagram marker in the subfigures (*f–h*). The arrows indicate the direction of movement along the closed orbit. The dynamics display two clearly disjoint time scales. All the subfigures are drawn using the fixed initial condition (0.3, 0.3, 0.3). (Online version in colour.)

trajectory evolves slowly within the neighbourhood of the interior saddle-focus E_7. We observe another different comparatively fast time scale that occurs when the trajectory leaves the vicinity of E_7. The existence of two such distinct time scales is ubiquitous in the atmosphere and oceanic dynamics.

This type of oscillatory dynamics can capture the beauty of governing eco-evolutionary dynamics. This spontaneous emergence of cyclical interaction gives the perfect window of opportunity for preserving biodiversity. These oscillatory states provide all strategies with a fair chance to survive. Although the temptation to defect is immense ($\beta = 2.60$), the coexistence of all competing strategies through cyclic dominance unfolds a surprising route to overcome the odds of the socio-ecological framework. Figure 5*e* contemplates how cooperators outcompete the defectors in a specific time window. However, in a different time window, the defectors overrule the punishers, who reduce the earnings of defectors by spending a part of their own resources. These punishers, in turn, outcompete the cooperators for a specific time span in figure 5*e*. In this way, any one of the three competitive strategies allows them all to coexist in the presence of a cyclic dominance. To ensure that the oscillatory dynamics of the system (2.10) remains physically meaningful, we plot $x + y + z$ as a function of time t in figure 5*d* and $x + y + z$ lies within [0, 1]. We also plot the individual periodic dynamics of x (red), y (magenta) and z (blue) in the subfigures (*a–c*) of figure 5.

(d) Evolutionary dynamics: a dynamical system approach

Until now we have inspected the evolutionary dynamics of the model (2.10) from the sole perspective of the evolutionary game dynamics. With the same motivation, we plot the
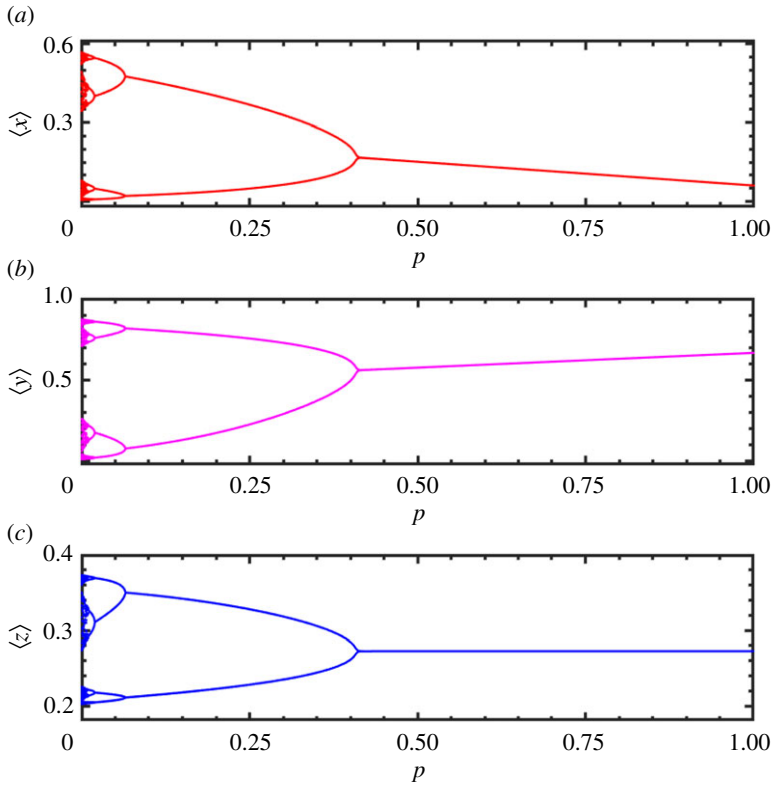
Figure 6. *Period-halving bifurcations with respect to the probability p: we plot the stationary point solutions of (a) $\langle x \rangle$, (b) $\langle y \rangle$ and (c) $\langle z \rangle$ for the set of parameter values $\sigma_1 = 0.55$, $\sigma_2 = 1.00$, $\sigma_3 = 0.70$, $\beta = 1.20$, $\delta = 0.30$, $\xi = 0.70$ and $\eta = 0.10$. We also plot their respective extrema for time-dependent solutions. The initial condition is kept fixed at $(0.3, 0.3, 0.3)$. We observe overcrowded solutions for $p < 0.4$ with $x + y + z > 1$. The remaining interval incorporates physically meaningful solutions with two different dynamical behaviours. For a suitable choice of p, the system converges to the interior stationary point E_7, indicating the stable coexistence of cooperators, punishers and defectors. Also, the periodic dynamics promote diverse coexisting strategies in the population. Punishers overcome the hurdle and become superior for $p \in [0.4, 0.407]$, where the temporal dynamics of all variables x, y and z are periodic. Although all strategies coexist maintaining diversity, the cooperators become inferior within this oscillating range as the inequality $y > z > x$ is identified. The proposed model allows a higher likelihood of playing the PD game with increasing p, which will become a conundrum for promoting cooperation. This expectation is reflected in the stationary state regime of $p \in (0.407, 1]$. (Online version in colour.)*

bifurcation diagram in figure 6 with respect to the parameter p for the set of parameter's values $\sigma_1 = 0.55$, $\sigma_2 = 1.00$, $\sigma_3 = 0.70$, $\beta = 1.20$, $\delta = 0.30$, $\xi = 0.70$ and $\eta = 0.10$. Here, $\langle x \rangle$, $\langle y \rangle$ and $\langle z \rangle$ indicate the relative fraction of cooperators, punishers and defectors, respectively. Thus,

$$\left. \begin{array}{l} \langle x \rangle = \dfrac{x}{x + y + z}, \\[2mm] \langle y \rangle = \dfrac{y}{x + y + z} \\[2mm] \langle z \rangle = \dfrac{z}{x + y + z}. \end{array} \right\} \tag{3.15}$$

and

Clearly, each of these relative fractions is defined only if $x + y + z = 1 - w \neq 0$. But since the population densities x, y and z are non-negative quantities, the only possibility to obtain $x + y + z = 0$ is $x = y = z = 0$. But the extinction stationary point E_0 is stable only when $\sigma_1, \sigma_2, \sigma_3 < \xi$, i.e. when the death rate surpasses the free space-induced benefits towards each
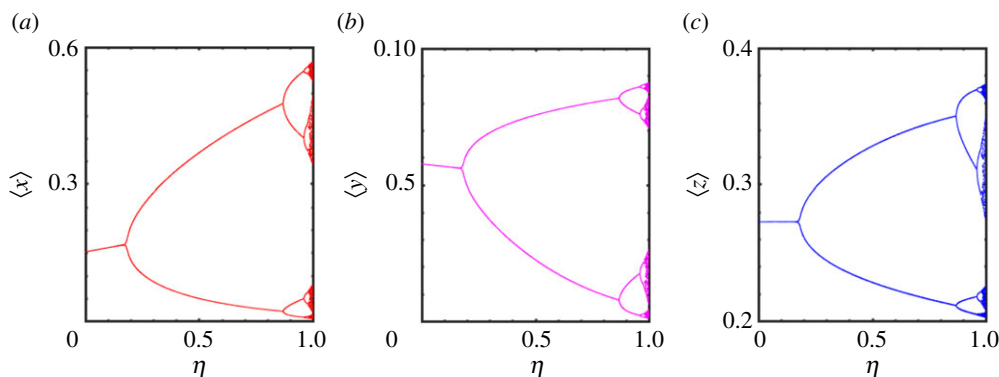
Figure 7. (*a–c*) *One parameter bifurcation diagrams with respect to η*: we observe a period-doubling bifurcation from the interior stationary point E_7 under the choice of parameter values $\sigma_1 = 0.55$, $\sigma_2 = 1.00$, $\sigma_3 = 0.70$, $\beta = 1.20$, $\delta = 0.30$, $\xi = 0.70$ and $p = 0.45$. We numerically identify a critical value $\eta_c \approx 0.20$ beyond which we obtain only an overcrowded solution, i.e. a bounded solution with $x + y + z > 1$. There are two types of solutions of system (2.10) within $\eta \in (0, 0.2]$. The first one indicates the coexistence of all strategies through the manifestation of the stationary point E_7 for $\eta \in (0, 0.186)$. At the same time, we recognize an oscillating solution for suitable values of $\eta \in [0.186, 0.2]$, such that the overall population density $x + y + z$ lies within the compact interval $[0, 1]$. This periodic attractor encourages the maintenance of diversity against the competition between different species. Here, eco-evolutionary dynamics are portrayed through the relative fraction of each subpopulation. For more details, see the main text. (Online version in colour.)

subpopulation. Figure 6 is drawn for the fixed initial condition $(0.3, 0.3, 0.3)$ and our choice of parameter values suggests E_0 is a saddle. Hence, E_0 is always unstable for this set of parametric values, and thus, (3.15) is well defined.

The system (2.10) experiences a period-halving bifurcation (i.e. inverse period-doubling) for the chosen parametric values and initial condition (figure 6). Here, the variation of p destroys a periodic orbit and creates a new periodic trajectory with half of the period of the earlier periodic orbit. Finally, the system settles down to the stable interior stationary point E_7. During the coexistence of all subpopulations (the stationary state E_7), punishers dominate the other subpopulations. To portray this prominent feature, we plot the bifurcation diagrams of each of the variables in figure 6*a–c*. Although we would like to mention there exist two distinct regimes in figure 6 based on overall population density. There exists a critical value of p_c beyond which we can possess $x + y + z \leq 1$. We numerically identify $p_c \approx 0.4$. Thus, even though our proposed model within $p \in [0, 0.4]$ provides fascinating dynamics, which are meaningful from the perspective of dynamical systems theory. But they are not physically meaningful from the aspect of evolutionary game theory, as the overall dynamics should lie within the closed and bounded interval $[0, 1]$ for a possible interpretation of our results. Within the interval $p \in [0.4, 1]$, the system displays oscillating behaviour for $p \in [0.4, 0.407]$ and constant vector (time-independent) solutions for $p \in (0.407, 1.0]$. The enhancement of p permits more likelihood for playing the PD game, where defection is more favourable. Thus, the dynamics of $\langle x \rangle$ (red) show a decreasing trend in the stationary state regime. However, the relative fraction of defectors $\langle z \rangle$ (blue) remains constant during this stationary point solution. Interestingly, the monotonic reduction of the relative fraction of cooperators facilitates the promotion of the relative fraction of punishers. $\langle y \rangle$ (magenta) displays the increasing tendency in figure 6*b* during the occurrence of E_7.

Similarly, we look into the qualitative changes of the solutions of the differential equations given in equation (2.10) with respect to the parameter η. We choose the same set of parameter values as considered in figure 6 with $p = 0.45$. We observe the emergence of a new periodic attractor with double the period from an existing periodic orbit in figure 7. Despite obtaining such complex dynamical features like period-doubling bifurcations, we have to explore only the solutions of system (2.10) within the interval $\eta \in (0, 0.2]$. For $\eta \leq \eta_c$ with $\eta_c \approx 0.2$, the overall

population density $x + y + z$ lies within the interval $[0, 1]$. Within this interval $(0, 0.2]$ of η, the system possesses periodic orbits and an interior stationary point E_7. The appearance of periodic attractors suggests that oscillations among different subpopulations provide flexibility for each strategy to survive. The stability of E_7 with increasing $\langle x \rangle$ (red) and decreasing $\langle y \rangle$ (magenta) is noticed in figure 7a,b. The fraction of defectors remains constant during this stationary state solution of the differential equations (2.10) as depicted through figure 7c. This type of constant behaviour of **D** is also observed in figure 3c. Although we have already provided an intuitive physical explanation behind the constant behaviour of the variable z in the interior stationary state regime in figures 3c and 6, we now present a justification behind this nature using the mathematical frame. We have already calculated each coordinate of $E_7 = (x^*, y^*, z^*)$ in equation (3.2). A careful inspection of z^* suggests z^* is a function of σ_1, σ_2, ξ and δ only. z^* does not depend on σ_3, p, η and β. Hence, we do not identify any change in the fraction of defectors in figures 6 and 7 within the interior stationary state regime, where we scrutinize the dynamics with respect to the variation of p and η.

Nevertheless, there is a thin difference in the obtained results between figures 3c and 7. Figure 3c depicts a decrease in the density of cooperators and an increase in the subpopulation of punishers. Figure 7 contemplates a reverse scenario in contrast to figure 3c. Yet, we consider the only difference in the values of parameters σ_1, β, and p between these two figures. Actually our choice of $p = 0.45$ gives $2p\eta - \eta = -0.1\eta$ for mutual defection. This reduced negative earning of defectors probably enhances the robustness of cooperation, which is reflected through figure 7a. This growing density of cooperators becomes the reason for decreasing punishers' density. Punishers are particular kinds of cooperators who try to sustain cooperation by preventing invasion by defectors. The fine δ from the payoff of defectors is deducted from their own resources. This sacrifice of punishers hampers the growth of punishers. The payoff for mutual defection in figure 3c is 0.1η, which is always positive. Even our mathematical analysis is also able to portray the same understanding. The choice of parameter values in figure 3c gives rise to the stabilization of the interior stationary point $E_7 = (x^*, y^*, z^*)$, where

$$\left. \begin{aligned} x^* &= \frac{5}{13} - \frac{\eta}{13}, \\ y^* &= \frac{\eta}{13} + \frac{1}{13} \\ z^* &= \frac{3}{13}. \end{aligned} \right\} \tag{3.16}$$

and

This indicates the gradual decrement of the fraction of cooperators and increment of the fraction of punishers with respect to η, which completely agrees with our numerical inspection shown in figure 3c. This also verifies our claim that the rate of reduction $(\eta/13)$ in the density of cooperators helps to promote the fraction of punishers by the same factor $(\eta/13)$. We can perform a similar analysis for figure 7 during the stabilization of the interior stationary point $E_7 = (x^*, y^*, z^*)$, where

$$\left. \begin{aligned} x^* &= \frac{5}{39} + \frac{\eta}{13}, \\ y^* &= -\frac{\eta}{13} + \frac{19}{39} \\ z^* &= \frac{3}{13}. \end{aligned} \right\} \tag{3.17}$$

and

Clearly, this validates the increasing nature of x^* and lessening of y^* with respect to η in figure 7, where the stationary point E_7 is stable. Again, the growth in x^* here by the term $\eta/13$ is the same as the rate of diminishing $\eta/13$ in y^*. A similar analysis can be supplemented for
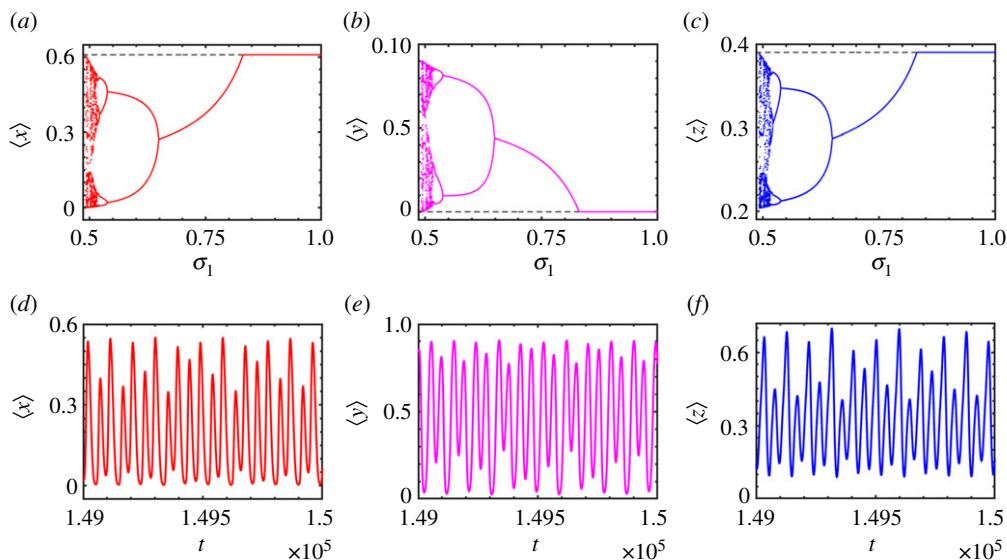
Figure 8. Boundary crisis: the effect of σ_1 on the fractions of cooperators $\langle x \rangle$, punishers $\langle y \rangle$ and defectors $\langle z \rangle$ are shown in (a), (b) and (c), respectively. For $0 < \sigma_1 \leq 0.49$, the attractor is annihilated. The dashed line denotes the relative density of each subpopulation for the unstable stationary point E_6. It collides with the chaotic attractor leading to sudden qualitative changes in chaotic dynamics of the system (2.10). The disappearance of the chaotic attractor is commonly known as boundary crisis. In the stationary state regime, we anticipate the enhancement of cooperator's density with increasing altruistic contribution of free space towards the cooperators. This expectation is fulfilled as C dominates D and P during the appearance of the stationary point E_6 in the subfigures (a–c). The simulation is carried out for 1.2×10^6 iterations. Parameters: $\sigma_2 = 1.00$, $\sigma_3 = 0.70$, $\beta = 1.20$, $\delta = 0.30$, $\xi = 0.70$, $\eta = 0.1$ and $p = 0.1$. (d–f) The chaotic time evolution of each relative fraction of subpopulation is plotted for $\sigma_1 = 0.515$. The simulation for these time evolutions is carried out for sufficiently long 1.5×10^7 iterations with fixed integration time-step $h = 0.01$. (Online version in colour.)

figure 6 during the occurrence of $E_7 = (x^*, y^*, z^*)$, where

$$
\left.\begin{array}{l}
x^* = \dfrac{8}{39} - \dfrac{2p}{13}, \\[2mm]
y^* = \dfrac{2p}{13} + \dfrac{16}{39} \\[2mm]
z^* = \dfrac{3}{13}.
\end{array}\right\} \tag{3.18}
$$

and

Note that all these equations (3.16)–(3.18) contain a constant solution $z^* = 3/13$ for the fraction of defectors.

Now we assess the influence of σ_1 in the eco-evolutionary dynamics of the proposed system (2.10). We set the values of the parameters $\sigma_2 = 1.00$, $\sigma_3 = 0.70$, $\beta = 1.20$, $\delta = 0.30$, $\xi = 0.70$, $\eta = 0.1$ and $p = 0.1$ to draw figure 8. This set of parametric values are the same as chosen in figure 6, where we plot the bifurcation diagram with respect to p with $\sigma_1 = 0.55$. We have already mentioned that the overall dynamics in figure 6 remains within $[0, 1]$ only for $p \geq 0.4$. So the choice of $p = 0.1$ in figure 8 may reveal many exciting outcomes. Since $\sigma_2 > \xi$, thus the extinction stationary point E_0 is unstable for our choice of parametric values. Hence, the relation (3.15) is well defined here too.

We vary $\sigma_1 \in (0, 1]$ to understand the importance of free space-induced benefits towards C. Here, we cannot trace numerically any bounded attractor for $\sigma_1 \in (0, 0.49]$. The bifurcation diagrams are drawn for 1.2×10^6 iterations with fixed initial condition $(0.3, 0.3, 0.3)$. In fact, for $\sigma_1 \to 0.49$, one can obtain an attractor which initially behaves chaotically for a possibly sufficiently long run, and finally, it will diverge leaving the signature of the transient chaos [109]. We choose

a value of $\sigma_1 = 0.515$, and run the system (2.10) for a massive number of iterations (1.5×10^7). The system exhibits chaotic dynamics, as shown in figure 8*d–f*. This dynamical behaviour changes through the period-halving bifurcation. Finally, the system converges to the stationary point $E_7 = (x^*, y^*, z^*)$, giving an opportunity for coexistence of each subpopulation. Here,

$$
x^* = \frac{17\sigma_1 - 26}{195(\sigma_1 - 1)},
$$
$$
y^* = \frac{266\sigma_1 - 221}{390(\sigma_1 - 1)}
$$

and

$$
z^* = \frac{3}{13}.
$$

(3.19)

This stationary point E_7 changes its stability beyond a critical value of σ_1, and then the system settles down to the punisher-free stationary point $E_6 = (\gamma_1, 0, \gamma_2)$, where

$$
\gamma_1 = \frac{39(10\sigma_1 - 7)}{10(64\sigma_1 - 39)}
$$

and

$$
\gamma_2 = \frac{5(10\sigma_1 - 7)}{2(64\sigma_1 - 39)}.
$$

(3.20)

In the entire stationary state E_7 regime, we expect a growth of the fraction of cooperators, as larger σ_1 facilitates the increase of $\langle x \rangle$ (red) through the selfless contribution of free space towards the cooperators. This fact is contemplated through figure 8*a*. Simultaneously the relative fraction of punishers $\langle y \rangle$ (magenta) is declining in figure 8*b*, and the relative fraction of defectors $\langle z \rangle$ (blue) is rising in figure 8*c*. We also plot the unstable position (black dashed lines) of the punisher-free stationary point E_6 using equation (3.20). During the appearance of E_6, $\langle x \rangle$, $\langle y \rangle$ and $\langle z \rangle$ reduce to 39/64, 0 and 25/64, respectively. Clearly, it indicates the dominance of **C** over **D** and **P**. We observe this unstable stationary point E_6 (black dashed line) coincides with the chaotic attractor, and consequently, the orbit will diverge. This boundary crisis through the variation of σ_1 leads to the destruction of a strange attractor within the interval $\sigma_1 \in (0, 0.49]$. One should note that the system dynamics provides overcrowded solutions for $\sigma_1 < 0.647$. Thus, the chaotic time series in figure 8*d–f* signifies the overcrowded solution with $x + y + z > 1$. Nevertheless, we acquire the physically meaningful solution of the system (2.10) from the perspective of the evolutionary game theory for $\sigma_1 \in [0.647, 1]$. This interval contains solutions of different characteristics, including periodic behaviour and stationary states (E_6 and E_7).

(e) A particular case with $\sigma_1 = \sigma_2 = \sigma_3 = \sigma$

Until now, we have investigated the system (2.10) with different sets of parametric values. But what if free space contributes the same amount of offering towards each of the subpopulations? To explore this inquiry, we take into consideration the relation $\sigma_1 = \sigma_2 = \sigma_3 = \sigma > 0$. Hence, the system (2.10) transforms to the following set of nonlinear equations:

$$
\dot{x} = x[(1 - \sigma)x + (1 - \sigma)y - \sigma z + (\sigma - \xi)],
$$
$$
\dot{y} = y[(1 - \sigma)x + (1 - \sigma)y - (\sigma + \delta)z + (\sigma - \xi)]
$$

and

$$
\dot{z} = z[(\beta - \sigma)x + (\beta - \delta - \sigma)y + (2p\eta - \eta - \sigma)z + (\sigma - \xi)].
$$

(3.21)

Here, $0 < \eta < 1$, $0 \leq p \leq 1$, $\beta > 1$ and $\delta, \xi, \sigma > 0$.

We perform a detailed analysis of this model (3.21), which is provided in table 2. Table 2 consists of three columns. The first column demonstrates different stationary points. The second column indicates the criteria for which each component of x, y and z along with the overall dynamics $x + y + z$ lies in [0, 1]. The eigenvalues of the Jacobian corresponding to each stationary point are explicitly calculated in the third column of table 2. The strictly negative real part of eigenvalues can address the stability of stationary points of the nonlinear differential equations (3.21).

Table 2. Existence and stability analysis of the stationary states for $\sigma_1 = \sigma_2 = \sigma_3 = \sigma$.

stationary points	existence	eigenvalues of the Jacobian
$E_0 = (0,0,0)$	Always	$\lambda_1 = \sigma - \xi, \lambda_2 = \sigma - \xi, \lambda_3 = \sigma - \xi$
$E_1 = \left(\dfrac{\xi-\sigma}{1-\sigma}, 0, 0\right)$ with $\sigma \neq 1$	$\sigma > \xi \geq 1$, or $0 < \sigma < \xi \leq 1$	$\lambda_1 = 0, \lambda_2 = \xi - \sigma, \lambda_3 = \dfrac{(\sigma-\xi)(\beta-1)}{\sigma-1}$
$E_2 = \left(0, \dfrac{\xi-\sigma}{1-\sigma}, 0\right)$ with $\sigma \neq 1$	$\sigma > \xi \geq 1$, or $0 < \sigma < \xi \leq 1$	$\lambda_1 = 0, \lambda_2 = \xi - \sigma, \lambda_3 = \dfrac{\xi - \sigma + \beta\sigma - \delta\sigma - \beta\xi + \delta\xi}{\sigma - 1}$
$E_3 = \left(0, 0, \dfrac{\xi-\sigma}{2p\eta - \eta - \sigma}\right)$ with $2p\eta - \eta - \sigma \neq 0$	If $(\xi - \sigma), (2p-1)\eta - \sigma > 0$, then $\sigma < \xi \leq (2p-1)\eta$. If $(\xi - \sigma), (2p-1)\eta - \sigma < 0$, then $\sigma > \xi \geq (2p-1)\eta$	$\lambda_1 = \xi - \sigma, \lambda_2 = \sigma - \xi - \dfrac{(\delta + \sigma)(\sigma - \xi)}{\eta + \sigma - 2p\eta}, \lambda_3 = \sigma - \xi - \dfrac{\sigma(\sigma - \xi)}{\eta + \sigma - 2p\eta}$
$E_4 = (\alpha_1, \alpha_2, 0)$, with $\alpha_1 + \alpha_2 = \dfrac{\xi - \sigma}{1-\sigma}$ and $\sigma \neq 1$	Either $\sigma > \xi > 1$ or $0 < \sigma < \xi < 1$. If $\xi = 1$, then $\alpha_1 + \alpha_2 = 1$	$\lambda_1 = \dfrac{(\beta - \sigma)(\xi - \sigma)}{1 - \sigma} - \delta\alpha_2 + (\sigma - \xi), \lambda_2 = 0, \lambda_3 = \xi - \sigma$
$E_5 = (0, \gamma_3, \gamma_4)$, where $\gamma_3 = \dfrac{\delta\sigma - \eta\sigma - \delta\xi + \eta\xi + 2p\eta\sigma - 2p\eta\xi}{\Delta_1}$ and $\gamma_4 = \dfrac{\sigma - \xi - \beta\sigma + \delta\sigma + \beta\xi - \delta\xi}{\Delta_1}$ with $\Delta_1 = \eta + \sigma - \beta\delta - 2p\eta - \beta\sigma + 2\delta\sigma - \eta\sigma + \delta^2 + 2p\sigma\eta \neq 0$	$0 < \gamma_3, \gamma_4 < 1$ and $0 < \gamma_3 + \gamma_4 \leq 1$	$\lambda_1 = \dfrac{\Delta}{\Delta_1}$, where $\Delta = \delta\sigma - \eta\sigma - \delta\xi + \eta\xi + \delta^2\sigma - \delta^2\xi - \beta\delta\sigma + \beta\eta\sigma - \delta\eta\sigma + \beta\delta\xi - \beta\eta\xi + \delta\eta\xi + 2p\eta\sigma - 2p\beta\eta\sigma + 2p\delta\eta\sigma + 2p\beta\eta\xi - 2p\delta\eta\xi$, $\lambda_2 = \dfrac{\delta\sigma - \delta\xi + \delta^2\sigma - \delta^2\xi - \beta\delta\sigma + \beta\delta\xi}{\Delta_1}, \lambda_3 = \xi - \sigma$
$E_6 = (\gamma_1, 0, \gamma_2)$ where $\gamma_1 = \dfrac{\eta\xi - \eta\sigma + 2p\eta\sigma - 2p\eta\xi}{\eta + \sigma - 2p\eta - \beta\sigma - \eta\sigma + 2p\eta\sigma}$ and $\gamma_2 = \dfrac{\sigma - \xi - \beta\sigma + \beta\xi}{\eta + \sigma - 2p\eta - \beta\sigma - \eta\sigma + 2p\eta\sigma}$ with $\eta + \sigma - 2p\eta - \beta\sigma - \eta\sigma + 2p\eta\sigma \neq 0$	$0 < \gamma_1, \gamma_2 < 1$ and $0 < \gamma_1 + \gamma_2 \leq 1$	$\lambda_1 = \xi - \sigma, \lambda_2 = \dfrac{\delta\xi - \delta\sigma + \beta\delta\sigma - \beta\delta\xi}{\eta + \sigma - 2p\eta - \beta\sigma - \eta\sigma + 2p\eta\sigma}, \lambda_3 = \dfrac{\eta\xi - \eta\sigma + \beta\eta\sigma - \beta\eta\xi + 2p\eta\sigma - 2p\eta\xi - 2p\beta\eta\sigma + 2p\beta\eta\xi}{\eta + \sigma - 2p\eta - \beta\sigma - \eta\sigma + 2p\eta\sigma}$

The computed eigenvalues can provide valuable insights into this model. For instance, the stationary point $E_1 = ((\xi - \sigma)/(1 - \sigma), 0, 0)$ with $\sigma \neq 1$ has the following eigenvalues: $\lambda_1 = 0$, $\lambda_2 = \xi - \sigma$ and $\lambda_3 = (\sigma - \xi)(\beta - 1)/(\sigma - 1)$. Now if $\lambda_2 > 0$, then this stationary point is unstable. If $\lambda_2 < 0$ then $\xi < \sigma$. Then the existence criteria reduces to only $\sigma > \xi \geq 1$. Now since $\beta - 1 > 0$, thus $\lambda_3 = (\sigma - \xi)(\beta - 1)/(\sigma - 1)$ is always positive. Hence in any circumstances, this stationary point is unstable if it exists.

This model (3.21) can be solved analytically if two of the coordinates of the initial fraction of the subpopulations (x_0, y_0, z_0) are zero. The solution with initial conditions $(x_0, 0, 0)$ and $x_0 \neq 0$ is

$$x = \frac{(\sigma - \xi)\Big(1 + \tanh\Big(c_1 + t\Big)\Big((\sigma/2) - (\xi/2)\Big)\Big)}{2(\sigma - 1)}, \quad y = 0 \text{ and } z = 0, \tag{3.22}$$

where c_1 is the initial condition-dependent constant. Similarly, we obtain the cooperator-free and defector-free solution with the initial condition $(0, y_0, 0)$ and $y_0 \neq 0$ as

$$x = 0, \quad y = \frac{(\sigma - \xi)\Big(1 + \tanh\Big(c_2 + t\Big)\Big((\sigma/2) - (\xi/2)\Big)\Big)}{2(\sigma - 1)} \quad \text{and } z = 0, \tag{3.23}$$

and the initial condition $(0, 0, z_0)$ with $z_0 \neq 0$ gives rise to the cooperator-free and punisher-free solution

$$x = 0, \quad y = 0 \quad \text{and } z = \frac{(\sigma - \xi)\Big(1 + \tanh\Big(c_3 + t\Big)\Big((\sigma/2) - (\xi/2)\Big)\Big)}{2(\eta + \sigma - 2\eta p)}, \tag{3.24}$$

where c_2 and c_3 are the initial condition-dependent constants.

One of the interesting findings is that this equally likely likelihood from free space leaves off the possibility of the manifestation of the interior stationary point E_7. This hindrance is also supported by equation (3.2). By inserting the constraint $\sigma_1 = \sigma_2 = \sigma_3 = \sigma$ in z^* of equation (3.2), we derive $z^* = 0$. Thus, it is impossible to obtain any interior stationary point with each of its coordinates being non-zero. However, we reckon seven stationary points have at least one of its coordinates being zero.

4. Concluding remarks

Competition among species for their existence and survivability [110–112] is a wicked problem in society under the realm of Darwin's theory of evolution. Besides, how cooperative behaviour evolves is one of the 25 big questions [113] facing science. Self-interested individuals are always interested in exploiting the cooperators leading to a challenging social dilemma for the persistence and emergence of cooperative behaviours. To understand the prevalence of cooperation in such an adverse scenario, we have formulated a mathematical model using the two paradigmatic games: PD and SD. These two two-person games yield two distinct outcomes. The PD game does not support cooperation, while the SD game supports stable coexistence of cooperative and non-cooperative behaviour. We introduce a parameter $p \in [0, 1]$, which indicates the probability of playing the PD game. The SD game is played with the complementary probability $(1 - p)$. We further extend the binary strategies: cooperation and defection by introducing a third one, *viz.* punishment. This punishing strategy helps to promote cooperation by reducing the earnings of defectors with a fine $\delta > 0$. However, these punishers are different from cooperators, as they have to bear an identical amount of cost δ for their punishment activities. Thus, they do not receive any additional benefits for promoting cooperation in competitive environments. In fact, they use their own resources for punishing defectors to control their self-centred mentality. Besides such inclusion of altruistic punishment in our evolutionary model (2.10), the free space is brought into play as an ecological variable. Free space selflessly provides replication opportunities to each subpopulation without any expectations. Instead of this charity, free space never claims any reciprocity. This one-sided contribution of free space without any self-benefit is brought into the limelight by introducing the variable w, and three different parameters σ_1, σ_2 and σ_3. All these

factors lead to fascinating outcomes in the evolutionary multi-game, which may provide valuable insights for understanding the evolution of cooperation in social systems.

We explain the results from the context of evolutionary game theory by applying the constraint $0 \leq x + y + z \leq 1$ so that the overall population dynamics presents physically meaningful inference. However, by doing this, we lose some captivating dynamics of our proposed model (2.10). Hence, we show some overcrowded solutions ($x + y + z > 1$) and explain those results using the well-known theories of nonlinear dynamics. These overcrowded solutions help us to illustrate why the solution diverges for some suitable set of parameters through the boundary crisis. Also, we can detect some parametric values for which the attractor exhibits a chaotic signature with $x + y + z > 1$. But our primary motivation is to explain the obtained results from the perspective of evolutionary game theory. Our proposed model can offer novel and meaningful conclusions on the evolution of various subpopulations with $x + y + z \in [0, 1]$. The model possesses eight different stationary points revealing several survivability and extinction possibilities. Although the interior stationary point does not exist, if free space decides to provide the same amount of benefits for all subpopulations. Insightful results can be captured using the appearance of the periodic attractor. The spontaneous emergence of oscillation describes the cyclic dominance sustaining the coexistence of three strategies under a suitable choice of parametric values. Our model has certain limitations, as our model yet cannot capture several real-life complexities. Our model contains eight different parameters impeding the exploration and analysis of the proposed model. Moreover, the system is multi-stable, displaying the sensitive dependence of the eco-evolutionary dynamics on initial fractions of subpopulations. These hindrances point out a more intensive investigation of the eco-evolutionary dynamics of the model proposed here. Still, we can contemplate the influence of each parameter through various numerical studies and interpret those results using the context of evolutionary game dynamics. We also validate our findings using analytical arguments. Mutation is one of the omnipresent phenomena in biology and eco-evolutionary dynamics. The evolutionary dynamics of multi-game are relatively ignored in most of the earlier studies on mutation [114–118]. Our results may reveal exciting findings on the inclusion of mutations. Analysing such replicator-mutator equations remains an important direction of future generalization, which is where our approach might unveil an even broader spectrum of attractive dynamical states. We conclude with the hope that instead of the complexity of the mathematical model, the evolutionary dynamics in different subpopulations may find diverse applicability well beyond the context studied here and will motivate some feasible scope of future research.

References

1. Perc M, Jordan JJ, Rand DG, Wang Z, Boccaletti S, Szolnoki A. 2017 Statistical physics of human cooperation. *Phys. Rep.* **687**, 1–51. (doi:10.1016/j.physrep.2017.05.004)
2. Nowak MA. 2006 Five rules for the evolution of cooperation. *Science* **314**, 1560–1563. (doi:10.1126/science.1133755)
3. Hammerstein P *et al.* 2003 *Genetic and cultural evolution of cooperation*. New York, NY: MIT press.
4. Capraro V, Perc M. 2018 Grand challenges in social physics: in pursuit of moral behavior. *Front. Phys.* **6**, 107. (doi:10.3389/fphy.2018.00107)

5. Darwin C. 1964 *On the origin of species: a facsimile of the first edition*, vol. 11. Cambridge, MA: Harvard University Press.
6. Hardin G. 2009 The tragedy of the commons. *J. Nat. Resour. Policy Res.* **1**, 243–253. (doi:10.1080/19390450903037302)
7. Chen X, Fu F. 2018 Social learning of prescribing behavior can promote population optimum of antibiotic use. *Front. Phys.* **6**, 139. (doi:10.3389/fphy.2018.00139)
8. Skutch AF. 1961 Helpers among birds. *Condor* **63**, 198–226. (doi:10.2307/1365683)
9. Chen X, Fu F. 2019 Imperfect vaccine and hysteresis. *Proc. R. Soc. B* **286**, 20182406. (doi:10.1098/rspb.2018.2406)
10. Seyfarth RM, Cheney DL. 1984 Grooming, alliances and reciprocal altruism in vervet monkeys. *Nature* **308**, 541–543. (doi:10.1038/308541a0)
11. Burns DA, Aherne J, Gay DA, Lehmann C. 2016 Acid rain and its environmental effects: recent scientific advances. *Atmos. Environ.* **146**, 1–4. (doi:10.1016/j.atmosenv.2016.10.019)
12. Wilkinson GS. 1984 Reciprocal food sharing in the vampire bat. *Nature* **308**, 181–184. (doi:10.1038/308181a0)
13. Nowak MA. 2006 *Evolutionary dynamics: exploring the equations of life*. Cambridge, MA: Harvard University Press.
14. Robert A *et al.* 1984 *The evolution of cooperation*. New York, NY: Basic Books.
15. Hofbauer J *et al.* 1998 *Evolutionary games and population dynamics*. Cambridge, UK: Cambridge University Press.
16. Smith JM. 1982 *Evolution and the theory of games*. Cambridge, UK: Cambridge University Press.
17. Weibull JW. 1995 *Evolutionary game theory*. Cambridge, MA: MIT Press.
18. Pennisi E. 2005 How did cooperative behavior evolve?. *Science* **309**, 93. (doi:10.1126/science.309.5731.93)
19. Von Neumann J, Morgenstern O. 2007 *Theory of games and economic behavior (commemorative edition)*. Princeton, NJ: Princeton University Press.
20. Smith JM, Price GR. 1973 The logic of animal conflict. *Nature* **246**, 15–18. (doi:10.1038/246015a0)
21. May RM, Leonard WJ. 1975 Nonlinear aspects of competition between three species. *SIAM J. Appl. Math.* **29**, 243–253. (doi:10.1137/0129022)
22. Perc M, Szolnoki A. 2010 Coevolutionary games–a mini review. *BioSystems* **99**, 109–125. (doi:10.1016/j.biosystems.2009.10.003)
23. Nowak MA, Komarova NL, Niyogi P. 2002 Computational and evolutionary aspects of language. *Nature* **417**, 611–617. (doi:10.1038/nature00771)
24. Nowak MA, May RM. 1994 Superinfection and the evolution of parasite virulence. *Proc. R. Soc. Lond. B* **255**, 81–89. (doi:10.1098/rspb.1994.0012)
25. Binmore KG. 1994 *Game theory and the social contract: just playing*, vol. 2. New York, NY: MIT press.
26. Kerr B, Riley MA, Feldman MW, Bohannan BJ. 2002 Local dispersal promotes biodiversity in a real-life game of rock–paper–scissors. *Nature* **418**, 171–174. (doi:10.1038/nature00823)
27. Axelrod R, Hamilton WD. 1981 The evolution of cooperation. *Science* **211**, 1390–1396. (doi:10.1126/science.7466396)
28. Rapoport A. 1966 *Two-person games: the essential ideas*. Ann Arbor, MI: University of Michigan Press.
29. Skyrms B. 2004 *The stag hunt and the evolution of social structure*. Cambridge, UK: Cambridge University Press.
30. Sigmund K, Hauert C, Nowak MA. 2001 Reward and punishment. *Proc. Natl Acad. Sci. USA* **98**, 10 757–10 762. (doi:10.1073/pnas.161155698)
31. Hauert C. 2010 Replicator dynamics of reward & reputation in public goods games. *J. Theor. Biol.* **267**, 22–28. (doi:10.1016/j.jtbi.2010.08.009)
32. Andreoni J, Harbaugh W, Vesterlund L. 2003 The carrot or the stick: rewards, punishments, and cooperation. *Am. Econ. Rev.* **93**, 893–902. (doi:10.1257/000282803322157142)
33. Fang Y, Benko TP, Perc M, Xu H, Tan Q. 2019 Synergistic third-party rewarding and punishment in the public goods game. *Proc. R. Soc. A* **475**, 20190349. (doi:10.1098/rspa.2019.0349)
34. Helbing D, Szolnoki A, Perc M, Szabó G. 2010 Defector-accelerated cooperativeness and punishment in public goods games with mutations. *Phys. Rev. E* **81**, 057104. (doi:10.1103/PhysRevE.81.057104)

35. Perc M. 2012 Sustainable institutionalized punishment requires elimination of second-order free-riders. *Sci. Rep.* **2**, 1–6. (doi:10.1038/srep00344)
36. Szolnoki A, Perc M. 2013 Effectiveness of conditional punishment for the evolution of public cooperation. *J. Theor. Biol.* **325**, 34–41. (doi:10.1016/j.jtbi.2013.02.008)
37. Sigmund K. 2007 Punish or perish? Retaliation and collaboration among humans. *Trends Ecol. Evol.* **22**, 593–600. (doi:10.1016/j.tree.2007.06.012)
38. Fehr E, Gächter S. 2002 Altruistic punishment in humans. *Nature* **415**, 137–140. (doi:10.1038/415137a)
39. Wang Z, Xia CY, Meloni S, Zhou CS, Moreno Y. 2013 Impact of social punishment on cooperative behavior in complex networks. *Sci. Rep.* **3**, 1–7. (doi:10.1038/srep03055)
40. Sasaki T, Okada I, Unemi T. 2007 Probabilistic participation in public goods games. *Proc. R. Soc. B* **274**, 2639–2642. (doi:10.1098/rspb.2007.0673)
41. Egas M, Riedl A. 2008 The economics of altruistic punishment and the maintenance of cooperation. *Proc. R. Soc. B* **275**, 871–878. (doi:10.1098/rspb.2007.1558)
42. Bell G. 2008 *Selection: the mechanism of evolution*. Oxford, UK: Oxford University Press on Demand.
43. De Silva H, Hauert C, Traulsen A, Sigmund K. 2010 Freedom, enforcement, and the social dilemma of strong altruism. *J. Evol. Econ.* **20**, 203–217. (doi:10.1007/s00191-009-0162-8)
44. Houston AI. 1993 Mobility limits cooperation. *Trends Ecol. Evol.* **8**, 194–196. (doi:10.1016/0169-5347(93)90096-8)
45. Tomassini M, Antonioni A. 2015 Lévy flights and cooperation among mobile individuals. *J. Theor. Biol.* **364**, 154–161. (doi:10.1016/j.jtbi.2014.09.013)
46. Nag Chowdhury S, Majhi S, Ozer M, Ghosh D, Perc M. 2019 Synchronization to extreme events in moving agents. *New J. Phys.* **21**, 073048. (doi:10.1088/1367-2630/ab2a1f)
47. Antonioni A, Tomassini M, Sánchez A. 2015 Short-range mobility and the evolution of cooperation: an experimental study. *Sci. Rep.* **5**, 1–9. (doi:10.1038/srep10282)
48. Premo LS, Brown JR. 2019 The opportunity cost of walking away in the spatial iterated prisoner's dilemma. *Theor. Popul. Biol.* **127**, 40–48. (doi:10.1016/j.tpb.2019.03.004)
49. Nag Chowdhury S, Kundu S, Duh M, Perc M, Ghosh D. 2020 Cooperation on interdependent networks by means of migration and stochastic imitation. *Entropy* **22**, 485. (doi:10.3390/e22040485)
50. Suzuki S, Kimura H. 2011 Oscillatory dynamics in the coevolution of cooperation and mobility. *J. Theor. Biol.* **287**, 42–47. (doi:10.1016/j.jtbi.2011.07.019)
51. Armano G, Javarone MA. 2017 The beneficial role of mobility for the emergence of innovation. *Sci. Rep.* **7**, 1–8. (doi:10.1038/s41598-017-01955-2)
52. Nag Chowdhury S, Majhi S, Ghosh D. 2020 Distance dependent competitive interactions in a frustrated network of mobile agents. *IEEE Trans. Netw. Sci. Eng.* **7**, 3159–3170. (doi:10.1109/TNSE.2020.3017495)
53. Zhang Y, Fu F, Chen X, Xie G, Wang L. 2015 Cooperation in group-structured populations with two layers of interactions. *Sci. Rep.* **5**, 1–13.
54. Wu T, Fu F, Wang L. 2011 Moving away from nasty encounters enhances cooperation in ecological prisoner's dilemma game. *PLoS ONE* **6**, e27669. (doi:10.1371/journal.pone.0027669)
55. Perc M, Wang Z. 2010 Heterogeneous aspirations promote cooperation in the prisoner's dilemma game. *PLoS ONE* **5**, e15117. (doi:10.1371/journal.pone.0015117)
56. Szolnoki A, Perc M, Szabó G. 2008 Diversity of reproduction rate supports cooperation in the prisoner's dilemma game on complex networks. *Eur. Phys. J. B* **61**, 505–509. (doi:10.1140/epjb/e2008-00099-7)
57. Szolnoki A, Szabó G. 2007 Cooperation enhanced by inhomogeneous activity of teaching for evolutionary Prisoner's Dilemma games. *Europhys. Lett.* **77**, 30004. (doi:10.1209/0295-5075/77/30004)
58. Szolnoki A, Perc M. 2009 Promoting cooperation in social dilemmas via simple coevolutionary rules. *Eur. Phys. J. B* **67**, 337–344. (doi:10.1140/epjb/e2008-00470-8)
59. Sugden R. 2004 *The economics of rights, co-operation and welfare*. Berlin, Germany: Springer.
60. Tayer M. 1987 *Possibility of cooperation: studies in rationality and social change*. Cambridge, UK: Cambridge University Press.
61. Scheuring I. 2005 The iterated continuous prisoner's dilemma game cannot explain the evolution of interspecific mutualism in unstructured populations. *J. Theor. Biol.* **232**, 99–104. (doi:10.1016/j.jtbi.2004.07.025)

62. Hauert C, Holmes M, Doebeli M. 2006 Evolutionary games and population dynamics: maintenance of cooperation in public goods games. *Proc. R. Soc. B* **273**, 2565–2571. (doi:10.1098/rspb.2006.3600)

63. Hendry AP. 2016 *Eco-evolutionary dynamics*. Princeton, NJ: Princeton University Press.

64. Hiltunen T, Ellner SP, Hooker G, Jones LE, Hairston Jr NG. 2014 Eco-evolutionary dynamics in a three-species food web with intraguild predation: intriguingly complex. *Adv. Ecol. Res.* **50**, 41–73. (doi:10.1016/b978-0-12-801374-8.00002-5)

65. Sigmund K, Holt RD. 2021 Toward ecoevolutionary dynamics. *Proc. Natl Acad. Sci. USA* **118**, e2100200118. (doi:10.1073/pnas.2100200118)

66. Hendry AP. 2019 A critique for eco-evolutionary dynamics. *Funct. Ecol.* **33**, 84–94. (doi:10.1111/1365-2435.13244)

67. Nag Chowdhury S, Kundu S, Banerjee J, Perc M, Ghosh D. 2021 Eco-evolutionary dynamics of cooperation in the presence of policing. *J. Theor. Biol.* **518**, 110606. (doi:10.1016/j.jtbi.2021.110606)

68. Pelletier F, Garant D, Hendry A. 2009 Eco-evolutionary dynamics. *Phil. Trans. R. Soc. B* **364**, 1483–1489. (doi:10.1098/rstb.2009.0027)

69. Brunner FS, Deere JA, Egas M, Eizaguirre C, Raeymaekers JA. 2019 *The diversity of eco-evolutionary dynamics: Comparing the feedbacks between ecology and evolution across scales*. New York, NY: Wiley Online Library.

70. Gokhale CS, Hauert C. 2016 Eco-evolutionary dynamics of social dilemmas. *Theor. Popul. Biol.* **111**, 28–42. (doi:10.1016/j.tpb.2016.05.005)

71. Wienand K, Frey E, Mobilia M. 2018 Eco-evolutionary dynamics of a population with randomly switching carrying capacity. *J. R. Soc. Interface* **15**, 20180343. (doi:10.1098/rsif.2018.0343)

72. Wang X, Zheng Z, Fu F. 2020 Steering eco-evolutionary game dynamics with manifold control. *Proc. R. Soc. A* **476**, 20190643. (doi:10.1098/rspa.2019.0643)

73. Fowler JH. 2005 Altruistic punishment and the origin of cooperation. *Proc. Natl Acad. Sci. USA* **102**, 7047–7049. (doi:10.1073/pnas.0500938102)

74. Szolnoki A, Szabó G, Perc M. 2011 Phase diagrams for the spatial public goods game with pool punishment. *Phys. Rev. E* **83**, 036101. (doi:10.1103/PhysRevE.83.036101)

75. Helbing D, Szolnoki A, Perc M, Szabó G. 2010 Evolutionary establishment of moral and double moral standards through spatial interactions. *PLoS Comput. Biol.* **6**, e1000758. (doi:10.1371/journal.pcbi.1000758)

76. Banerjee J, Layek RK, Sasmal SK, Ghosh D. 2019 Delayed evolutionary model for public goods competition with policing in phenotypically variant bacterial biofilms. *Europhys. Lett.* **126**, 18002. (doi:10.1209/0295-5075/126/18002)

77. Wang Z, Szolnoki A, Perc M. 2014 Different perceptions of social dilemmas: evolutionary multigames in structured populations. *Phys. Rev. E* **90**, 032813. (doi:10.1103/PhysRevE.90.032813)

78. Qin J, Chen Y, Kang Y, Perc M. 2017 Social diversity promotes cooperation in spatial multigames. *Europhys. Lett.* **118**, 18002. (doi:10.1209/0295-5075/118/18002)

79. Szolnoki A, Perc M. 2014 Coevolutionary success-driven multigames. *Europhys. Lett.* **108**, 28004. (doi:10.1209/0295-5075/108/28004)

80. Szolnoki A, Mobilia M, Jiang LL, Szczesny B, Rucklidge AM, Perc M. 2014 Cyclic dominance in evolutionary games: a review. *J. R. Soc. Interface* **11**, 20140735. (doi:10.1098/rsif.2014.0735)

81. Czárán TL, Hoekstra RF, Pagie L. 2002 Chemical warfare between microbes promotes biodiversity. *Proc. Natl Acad. Sci. USA* **99**, 786–790. (doi:10.1073/pnas.012399899)

82. Reichenbach T, Mobilia M, Frey E. 2007 Mobility promotes and jeopardizes biodiversity in rock–paper–scissors games. *Nature* **448**, 1046–1049. (doi:10.1038/nature06095)

83. Sinervo B, Lively CM. 1996 The rock–paper–scissors game and the evolution of alternative male strategies. *Nature* **380**, 240–243. (doi:10.1038/380240a0)

84. Szolnoki A, Perc M. 2016 Biodiversity in models of cyclic dominance is preserved by heterogeneity in site-specific invasion rates. *Sci. Rep.* **6**, 1–9. (doi:10.1038/s41598-016-0001-8)

85. Perc M, Szolnoki A, Szabó G. 2007 Cyclical interactions with alliance-specific heterogeneous invasion rates. *Phys. Rev. E* **75**, 052102. (doi:10.1103/PhysRevE.75.052102)

86. Gilg O, Hanski I, Sittler B. 2003 Cyclic dynamics in a simple vertebrate predator-prey community. *Science* **302**, 866–868. (doi:10.1126/science.1087509)

87. Elowitz MB, Leibler S. 2000 A synthetic oscillatory network of transcriptional regulators. *Nature* **403**, 335–338. (doi:10.1038/35002125)

88. Camassa R. 1995 On the geometry of an atmospheric slow manifold. *Physica D* **84**, 357–397. (doi:10.1016/0167-2789(94)00239-M)

89. Arnold L. 1995 Random dynamical systems. In *Dynamical systems* (ed. R Johnson), pp. 1–43. Berlin, Germany: Springer.

90. Nag Chowdhury S, Ghosh D. 2020 Hidden attractors: a new chaotic system without equilibria. *Eur. Phys. J. Spec. Top.* **229**, 1299–1308. (doi:10.1140/epjst/e2020-900166-7)

91. Koseska A, Volkov E, Kurths J. 2013 Oscillation quenching mechanisms: amplitude vs. oscillation death. *Phys. Rep.* **531**, 173–199. (doi:10.1016/j.physrep.2013.06.001)

92. Dixit S, Nag Chowdhury S, Ghosh D, Shrimali MD. 2021 Dynamic interaction induced explosive death. *Europhys. Lett.* **133**, 40003. (doi:10.1209/0295-5075/133/40003)

93. Ray A, Kundu S, Ghosh D. 2020 Aging transition in weighted homogeneous and heterogeneous networks. *Europhys. Lett.* **128**, 40002. (doi:10.1209/0295-5075/128/40002)

94. Dixit S, Nag Chowdhury S, Prasad A, Ghosh D, Shrimali MD. 2021 Emergent rhythms in coupled nonlinear oscillators due to dynamic interactions. *Chaos* **31**, 011105. (doi:10.1063/5.0039879)

95. Kundu S, Majhi S, Ghosh D. 2018 Resumption of dynamism in damaged networks of coupled oscillators. *Phys. Rev. E* **97**, 052313. (doi:10.1103/PhysRevE.97.052313)

96. Nag Chowdhury S, Ghosh D, Hens C. 2020 Effect of repulsive links on frustration in attractively coupled networks. *Phys. Rev. E* **101**, 022310. (doi:10.1103/PhysRevE.101.022310)

97. Saxena G, Prasad A, Ramaswamy R. 2012 Amplitude death: the emergence of stationarity in coupled nonlinear systems. *Phys. Rep.* **521**, 205–228. (doi:10.1016/j.physrep.2012.09.003)

98. Nowak MA, May RM. 1992 Evolutionary games and spatial chaos. *Nature* **359**, 826–829. (doi:10.1038/359826a0)

99. Nowak MA, May RM. 1993 The spatial dilemmas of evolution. *Int. J. Bifurcation Chaos* **3**, 35–78. (doi:10.1142/S0218127493000040)

100. Pearce MT, Agarwala A, Fisher DS. 2020 Stabilization of extensive fine-scale diversity by ecologically driven spatiotemporal chaos. *Proc. Natl Acad. Sci. USA* **117**, 14 572–14 583. (doi:10.1073/pnas.1915313117)

101. Sanders JB, Farmer JD, Galla T. 2018 The prevalence of chaotic dynamics in games with many players. *Sci. Rep.* **8**, 1–13. (doi:10.1038/s41598-018-22013-5)

102. Mukhopadhyay A, Chakraborty S. 2020 Deciphering chaos in evolutionary games. *Chaos* **30**, 121104. (doi:10.1063/5.0029480)

103. Grebogi C, Ott E, Yorke JA. 1987 Chaos, strange attractors, and fractal basin boundaries in nonlinear dynamics. *Science* **238**, 632–638. (doi:10.1126/science.238.4827.632)

104. Grebogi C, Ott E, Yorke JA. 1983 Crises, sudden changes in chaotic attractors, and transient chaos. *Physica D* **7**, 181–200. (doi:10.1016/0167-2789(83)90126-4)

105. Grebogi C, Ott E, Yorke JA. 1982 Chaotic attractors in crisis. *Phys. Rev. Lett.* **48**, 1507. (doi:10.1103/PhysRevLett.48.1507)

106. Taylor PD, Jonker LB. 1978 Evolutionary stable strategies and game dynamics. *Math. Biosci.* **40**, 145–156. (doi:10.1016/0025-5564(78)90077-9)

107. Kelso JS. 2012 Multistability and metastability: understanding dynamic coordination in the brain. *Phil. Trans. R. Soc. B* **367**, 906–918. (doi:10.1098/rstb.2011.0351)

108. Pisarchik AN, Jaimes-Reátegui R, Sevilla-Escoboza R, Huerta-Cuellar G, Taki M. 2011 Rogue waves in a multistable system. *Phys. Rev. Lett.* **107**, 274101. (doi:10.1103/PhysRevLett.107.274101)

109. Lai YC, Tél T. 2011 *Transient chaos: complex dynamics on finite time scales*, vol. 173. Berlin, Germany: Springer Science & Business Media.

110. Murray JD. 2007 *Mathematical biology: I. An introduction*, vol. 17. Berlin, Germany: Springer Science & Business Media.

111. Kundu S, Majhi S, Sasmal SK, Ghosh D, Rakshit B. 2017 Survivability of a metapopulation under local extinctions. *Phys. Rev. E* **96**, 062212. (doi:10.1103/PhysRevE.96.062212)

112. Kundu S, Majhi S, Ghosh D. 2021 Persistence in multilayer ecological network consisting of harvested patches. *Chaos* **31**, 033154. (doi:10.1063/5.0047221)

113. Kennedy D, Norman C. 2005 What don't we know. *Science* **309**, 75. (doi:10.1126/science.309.5731.75)

114. Mobilia M. 2010 Oscillatory dynamics in rock–paper–scissors games with mutations. *J. Theor. Biol.* **264**, 1–10. (doi:10.1016/j.jtbi.2010.01.008)

115. Toupo DF, Strogatz SH. 2015 Nonlinear dynamics of the rock-paper-scissors game with mutations. *Phys. Rev. E* **91**, 052907. (doi:10.1103/PhysRevE.91.052907)

116. Toupo DF, Rand DG, Strogatz SH. 2014 Limit cycles sparked by mutation in the repeated prisoner's dilemma. *Int. J. Bifurcation Chaos* **24**, 1430035. (doi:10.1142/S0218127414300353)

117. Duong MH *et al.* 2020 On equilibrium properties of the replicator–mutator equation in deterministic and random games. *Dyn. Games Appl.* **10**, 641–663. (doi:10.1007/s13235-019-00338-8)

118. Mittal S, Mukhopadhyay A, Chakraborty S. 2020 Evolutionary dynamics of the delayed replicator-mutator equation: limit cycle and cooperation. *Phys. Rev. E* **101**, 042410. (doi:10.1103/PhysRevE.101.042410)

28

royalsocietypublishing.org/journal/rspa *Proc. R. Soc. A* **477**: 20210397